Technical

Report

Semi-Annual Report
SA-B2368-4

COLD WELDING OF COPPER UNDER ULTRAHIGH VACUUM

by

H. Conrad
L. Rice

October 1, 1966 to March 31, 1967

Sponsored by

OFFICE OF NAVAL RESEARCH

Contract Nonr 4825(00)
NR 031-708

THE FRANKLIN INSTITUTE RESEARCH LABORATORIES
BENJAMIN FRANKLIN PARKWAY • PHILADELPHIA, PENNA. 19103

COLD WELDING OF COPPER UNDER ULTRAHIGH VACUUM

H. Conrad and L. Rice

The Franklin Institute Research Laboratories
Philadelphia, Pa.

for presentation and publication

ASTM-ASME Symposium Adhesion of Materials
in Space Environments

Toronto, Canada
May 1-2, 1967

Research Sponsored by
Office of Naval Research
Contract Nonr 4825(00)

COLD WELDING OF COPPER UNDER ULTRAHIGH VACUUM

H. Conrad and L. A. Rice
The Franklin Institute Research Laboratories

ABSTRACT

The cohesion of copper under ultrahigh vacuum in the range 10^{-11} to 10^{-9} torr was investigated using the technique of cold welding specimens previously fractured in the vacuum. It was found that the cohesion coefficient increased with the compressive load during cold welding but was relatively independent of the purity and structure of the copper (and in turn the hardness and strength), time of contact over the range 5 sec to 900 sec and exposure to the vacuum environment over the range of 10^{-9} to 10^{-4} torr-sec.

No voids were detected at magnifications up to 1000X along the weld interface of fine-grained (6 - 10 μ) specimens which had been cold welded at loads approaching the virgin fracture load. Voids were, however, observed for coarse-grained (100 - 450 μ) specimens at such loads and for all specimens at loads appreciably below the initial fracture load. From ultrasonic transmission studies it was deduced that the cohesive strength was proportional to the area of contact developed during cold welding.

The effect of compressive load on the cohesive strength is explained by the increase in contact area resulting from elastic and plastic strains in the vicinity of the interface. This interpretation suggests that the cohesion coefficient should be proportional to the reciprocal of the elastic modulus, which was shown to be the case when comparing Cu, Ag and Fe. The fact that the cohesion coefficient was independent of exposure to the vacuum environment up to 10^{-2} torr-sec is shown to be in accord with adsorption theories.

COLD WELDING OF COPPER UNDER ULTRAHIGH VACUUM

H. Conrad and L. Rice

INTRODUCTION

From a technological viewpoint, an understanding of the cohesion (or adhesion[†]) of metals is important to such areas as friction and wear and bonding, joining and cladding. Especially important in recent years has become the subject of the cohesion of metals in ultrahigh vacuum (defined here as a pressure < 10^{-8} torr[(1)]) as related to the behavior of components and systems in a space environment and the possibility of joining materials in space by cold welding.[(2)] Besides having a direct bearing on technology, studies of the cohesion of metals can also provide information concerning the nature and behavior of surfaces, which is of value to understanding such phenomena as catalysis, oxidation and corrosion.

The objective of the present research program is to develop a better understanding of the cohesion of metals through a study of cold welding under ultrahigh vacuum. It was decided to investigate the cold welding of copper initially, since a considerable amount of basic data on the crystal lattice properties, surface properties and mechanical properties of this metal are already available and since only a limited amount of data on the cohesion of this metal in ultrahigh vacuum had been previously published.[(2-4)]

[†]The term cohesion will be used to refer to the bonding of a metal to itself, while adhesion will be used for dissimilar metals.

Since in cohesion studies it is desirable to obtain surfaces which are free of contaminating gases or films, it was decided to investigate the cohesion of specimens which had been fractured in a vacuum, similar to the experiments of Ham.[3,4] In this way, clean surfaces can be produced with relative ease and the results obtained with them will provide a reference for comparison with those from surfaces previously contaminated and subsequently cleaned by various means. The present paper thus describes the results obtained on the cold welding under ultrahigh vacuum of previously fractured copper specimens.

EXPERIMENTAL PROCEDURE

The material employed in the present studies was polycrystalline copper of three impurity contents: commercial tough pitch, commercial OFHC and high purity (99.999%) copper from American Smelting and Refining Company. Cold welding studies were conducted on various conditions of these materials, representing a range of structures, grain sizes, and mechanical properties; see Table I and Figures 1 to 3.

To localize the fracture and to reduce the amount of necking, a notched specimen of the form shown in Fig. 4 was employed. This specimen has a notch geometry and notch sharpness ($r/\rho = 5.0$) similar to those used by Ham[3,4] and represents the optimum for obtaining a relatively flat fracture with the load at fracture being least sensitive to small changes in notch geometry.[5] Specimens of the form shown in Fig. 4 were machined from the as-received rod, electropolished† and either tested directly, or

†Electropolishing solution: 80 ml H_2O, 40 ml ethanol, 60 ml H_3PO_4; 9 - 10 volts at 25°C.

annealed in a vacuum of 10^{-6} torr to produce the desired grain size, electropolished again and tested.

The cold welding tests were conducted in the ultrahigh vacuum testing apparatus shown schematically in Fig. 5. This system is capable of producing a vacuum of 2×10^{-11} torr and applying a maximum load in tension or compression of 1000 lbs. with a load sensitivity of 0.01 lb. and an elongation sensitivity of 2×10^{-4} in. To be able to apply both tensile and compressive loads to the specimen and to ensure good mating of the two fracture surfaces, the gripping and alignment fixture shown in Fig. 6 was employed.

Previous to conducting the cohesion studies, the mechanical testing machine was calibrated using a hardened steel rod. This established the elastic behavior of the machine (which was relatively soft) and provided corrections which could be applied to the test data to separate machine effects from the behavior of the specimen. The bellows are so arranged that no corrections were needed to account for their contraction or expansion. Specimen elongations were all measured from the crosshead motion of the testing machine.

A cohesion test consisted of pulling a specimen to fracture at a constant crosshead velocity of 0.01 in. per min. under an ultrahigh vacuum† (after initially flushing the system with purified dry nitrogen†† and

---

†The vacuums investigated were in the range 2×10^{-11} to 2×10^{-9} torr; however, most tests were conducted in the range of 2×10^{-11} to 10×10^{-11} torr.

††The purified nitrogen contained 0.001 wt.% O_2 and 0.0012 wt.% H_2O maximum.

baking out at 150°C), exposing the fracture surfaces to the vacuum environment for a predetermined time, pushing the two fractured halves together at the same crosshead speed and to a fixed load, holding the specimen at the maximum load for a fixed time†, and finally pulling the cold welded specimen apart again (at the same crosshead speed) to ascertain the fracture load of the cold welded specimen; i.e., the degree of cohesion. All tests were conducted at room temperature.

In an attempt to establish the area of contact nondestructively, some of the specimens were removed from the vacuum chamber following cold welding and examined at ambient pressure with a Sperry UM 715 reflectroscope, using the "through transmission technique" with one search unit being applied to each end of the test specimen. In this technique the transmitting search unit projects an ultrasonic beam into the specimen which travels through the material to the opposite surface where it is picked up by the receiving search unit. Any discontinuities in the path of the beam will cause a reduction in the energy passing through the specimen to the receiving search unit. Contact between the search crystals and the specimen ends was established using a thin film of glycerin.

A limited microscopic study was made of the nature and structure of the weld interface after cold welding. For this study, specimens were cold welded under the ultrahigh vacuum and then removed from the chamber, sectioned and prepared for metallographic examination using standard procedures.

†The time of contact was varied from 5 to 900 seconds, however most tests were conducted with a contact time of 300 seconds.

EXPERIMENTAL RESULTS

1. Mechanical Tests

Examples of the load versus crosshead travel curves obtained in the present tests under ultrahigh vacuum are given in Figs. 7-9. The curves of Fig. 7 are representative of specimens which were in the cold worked state prior to testing while those of Figs. 8 and 9 are typical for annealed specimens. The mechanical properties under ultrahigh vacuum derived from these curves for the initial loading are given in Table I and are similar to those for specimens tested at atmospheric pressure, differing from the results reported for aluminum[6].

Evident from Figs. 7-9 is that during the cold welding phase of the load-crosshead travel curves a departure from the linear "elastic" region of the curves occurs for loads in excess of about $R_c (= L_c/L_{F_o}) = 0.5$, suggesting the occurrence of plastic flow. This plastic component of the contraction $\Delta\ell_p$ ($= \Delta\ell_t - \Delta\ell_E$) was found to be approximately proportional to $(L_c/L_{F_o})^3$; see Fig. 10. $\Delta\ell_t$ is the total contraction; $\Delta\ell_E$ is the "elastic" contraction derived from a projection of the linear region of the load versus crosshead travel curve; L_c and L_{F_o} are defined in Figs. 7-9.

One way of comparing the cohesion data on the various coppers, which only involves measurements of loads and therefore does not include any errors which may be associated with area determinations, is to plot the cohesion ratio $R_F (= L_{F_1}/L_{F_o})$ versus the compression ratio $R_c (= L_c/L_{F_o})$. Again, the significance of L_{F_1}, L_{F_o} and L_c is indicated in Figs. 7-9. A plot of R_F versus R_c for the tough pitch copper specimens is presented in Fig. 11; a similar plot for all materials tested is given in Fig. 12.

Evident from these figures is that the cohesion ratio increases with the compression ratio, essentially independent of structure, purity, and the contact time at the maximum compressive load. Also to be noted is that the R_F versus R_c curves are not linear but exhibit a slight positive curvature. This feature is further revealed in Fig. 13 where the cohesion coefficient α ($= L_{F_1}/L_c$) is plotted versus the compression ratio. It is here seen that α can be considered to increase linearly with R_c yielding

$$\alpha = \alpha_o + \beta R_c \qquad (1)$$

with $\alpha_o = 0.75$ and $\beta = 0.15$.

An alternate method of comparing the cold welding results is illustrated in Fig. 14, where the "average" cohesion stress σ_F ($= L_{F_1}/A_{F_1}$) is plotted versus the "average" compression stress σ_c ($= L_c/A_{F_1}$). A_{F_1} is the area after fracture of the cold welded specimen. The data of Fig. 14 indicate that the cohesion stress is approximately proportional to the compression stress, yielding $\alpha_{av} = \sigma_F/\sigma_c = 0.86$. However, from Fig. 15 it is seen that, by plotting σ_F/σ_c for each test, the value of α increases with stress from about 0.63 - 0.83 at low stresses to 0.80 - 1.0 at 80 ksi and thereafter remains essentially constant, indicating a slight positive curvature at low stresses in the curve of Fig. 14.

The effect of exposure of the fractured surfaces to the vacuum environment prior to cold welding is illustrated in Fig.16, where α_o is plotted versus the exposure. α_o was derived for each test through Eq. 1. The pressure and time ranges covered to yield these exposures was 2×10^{-11} torr

to 2×10^{-9} torr and 37 sec to 6×10^{5} sec respectively. The results for a given exposure were independent of the pressure and time, over the range considered. Evident from Fig. 16 is that the cohesion coefficient is independent of exposure up to 10^{-4} torr-sec. Significant in this regard is that for a sticking coefficient of 1.0, a monolayer of gas would form after an exposure of about 2×10^{-6} torr-sec.[7]

2. Ultrasonic Tests

The results of the measurements of the transmission of ultrasonic waves through the cold welded specimens of tough pitch copper are presented in Fig. 17, which indicates that the transmitted wave amplitude is proportional to the cohesion ratio R_F. Assuming that the amplitude of the transmitted wave is proportional to the area of contact along the weld interface A_w, the results of Fig. 17 suggest that

$$R_c = \sigma_{F_1} / \sigma_{F_o} \simeq \frac{A_w}{A_{F_c}} \qquad (2)$$

where A_{F_o} is the fracture area for the initial loading of the specimen.

3. Microscopic Study

The photomicrograph of Fig. 18 illustrates the appearance of the weld interface near the center of a cold welded tough pitch copper specimen, when viewed in the unetched condition. Porosity is noted along the interface for a compression ratio $R_c = 0.5$, while there is no indication of voids for $R_c = 1.0$ at the magnification shown or higher (up to 1000X). Similar behavior was noted for the fine-grained (6μ) OFHC specimens. However,

the coarse-grained OFHC (100μ) and coarse grained high purity (450μ) specimens exhibited slight porosity even for R_c = 1.0, with the amount of porosity increasing with decrease in R_c. At the time of this writing, no microstructure analysis had been made of welded specimens of the cold worked materials.

The appearance of the weld interface for R_c = 1.0 after etching is illustrated in Figs. 19-21. The excellent mating of the two fracture surfaces possible with the present apparatus is revealed in Fig. 19. Note here, for example, the good matching of grain boundaries and twin boundaries across the weld interface. Comparing Figs. 19 and 20 with Fig. 18 reveals that the matching of the two fractured surfaces did not occur as well for the OFHC copper specimens as for the tough pitch copper. However, the results of Figs. 12 and 13 indicate that the degree of matching had only a slight influence, if any, on the cohesion.

DISCUSSION

A significant finding of the present results is that the cohesion of copper is independent of purity and structure (cold work and grain size) and in turn independent of strength and hardness, over the range considered. This is contrary to the idea that cohesion (or adhesion) may be directly related to the strength or hardness of the materials which are cold welded.[8-10]

The cohesion coefficient α obtained in the present tests increased with the compression ratio R_c, or with the compression stress σ_c. A linear

increase of α with R_c indicated in Fig. 13 can be explained as follows: Assuming that the fracture stress of the cold welded copper specimens is proportional to the area of contact (which is in accord with the ultrasonic transmission results of Fig. 17), then it seems reasonable that

$$L_{F_i}/A_w \cong L_{F_o}/A_{F_o} \tag{3}$$

where L_{F_o} and A_{F_o} are the load and area at fracture of the virgin specimen and L_{F_i} and A_w are the load and true area of contact along the interface of the cold welded specimen. Moreover, it is expected that the area of contact A_w developed during cold welding will depend on the compressive load and as a first approximation is given by

$$\frac{A_w}{A_o} = a + b\,\varepsilon_E + c\,\varepsilon_p \tag{4}$$

where a represents the contribution at zero stress, $b\,\varepsilon_E$ represents the contribution due to the elastic strains at the weld interface and $c\,\varepsilon_p$ represents that due to plastic strains.

Elastic considerations suggest that

$$b\,\varepsilon_E \cong \frac{b_1}{E}\left(\frac{L_c}{L_{F_o}}\right) \tag{5}$$

where E is the elastic modulus. Moreover, since a parabolic stress strain behavior is often observed for both plastic microstrain[11,12] and

macrostrain,[13,14] a reasonable assumption for the plastic contribution appears to be

$$c\,\varepsilon_p \cong \frac{c_1}{E^2}\left(\frac{L_c}{L_{F_o}}\right)^2 \tag{6}$$

Inserting Eqs. 4-6 into eqs. 3 and 4 and rearranging gives

$$L_{F_1}/L_c \cong \frac{b_1}{E} + \frac{c_1}{E^2}\left(\frac{L_c}{L_{F_o}}\right) \tag{7}$$

when a/L_{F_o} is small, which is expected in the present case. Eq. 7 is in accord with the linear relationship between R_F and R_c indicated in Fig. 13.

On the other hand, the results of Fig. 10 suggest that the quantity $c\,\varepsilon_p$ may be more nearly given by

$$c\,\varepsilon_p \cong \frac{c_2}{E^3}\left(\frac{L_c}{L_{F_o}}\right)^3 \tag{8}$$

Inserting Eq. 8 into Eqs. 3 and 4 and rearranging gives

$$L_F/L_c \cong \frac{b_1}{E} + \frac{c_2}{E^3}\left(\frac{L_c}{L_{F_o}}\right)^2 \tag{9}$$

which requires that the cohesion ratio R_F increase linearly with the square of the compression ratio R_c. That the present data can also be considered

to obey Eq. 9 is illustrated in Fig. 22. The straight line drawn here gives

$$\alpha = 0.80 + 0.10\ R_c^2 \tag{10}$$

The present results do not permit a separation between a linear or parabolic relation between α and R_c.

It is of interest to compare the values of the cohesion coefficient α obtained in the present tests with those obtained by other investigators for copper,[3,4] silver[15] and iron.[4] From Ham's data,[3,4] one obtains for OFHC copper $\alpha = 0.62 - 0.68$ at 90°C for an exposure of 2×10^{-6} torr-sec ($p = 5 \times 10^{-10}$ torr) and compressive stresses of 35 - 52 Ksi. These are in reasonable accord with the results presented here. Keller's data[15] for silver cleaned by argon ion bombardment and contacted in a vacuum of 10^{-10} torr at room temperature yield $\alpha = 0.84$, while Ham's data[3,4] for steel yields $\alpha = 0.34 - 0.36$ at 25°C for exposures of 6×10^{-8} to 6×10^{-7} torr-sec and compressive stresses of 60-90 Ksi. From Table II it is seen that the product αE (E = Young's modulus) is approximately a constant for these metals, suggesting that the lower values of α for steel compared to copper and silver are due to the difference in modulus rather than a difference in crystal structure. An approximately constant value of αE is expected on the basis of Eqs. 7 and 9, especially when α_o ($= b_1/E$) represents a large part of α.

Sikorski[8,9] has shown that when comparing different metals the median cohesion coefficient tends to decrease with increase in strength

or hardness. This is in accord with the above analysis, for there is both theoretical and experimental support[13] that the hardness and strength of metals increases with increase in modulus. Thus, since according to Eqs. 7 and 9 α is inversely related to the modulus, one expects a decrease in α with increase in strength or hardness when comparing different metals, but not for the same metal. It should be pointed out that the relationship between α and strength (or hardness) for different metals may be complicated, for the relationship between strength and modulus is not always simple, especially when comparing metals of different crystal structures.

The observation that the cohesion coefficient was independent of exposure to the vacuum environment up to exposures of 10^{-4} torr-sec will now be considered. Since the system was initially flushed with high purity nitrogen, it is expected that this gas is the major constituent in the vacuum environment, other than possibly the inert gases. Theoretical considerations and experimental observations[1,16] indicate that nitrogen does not adsorb on copper at the pressures and temperatures of the present investigation. Hence, an exposure of 10^{-4} torr-sec to this gas is not expected to influence the cohesion. Furthermore, if one assumes that the fraction of oxygen and water molecules in the vacuum is the same as that in the original nitrogen gas (approximately 0.001 wt. %), the maximum exposure of 10^{-4} torr-sec to the vacuum environment would only represent

an equivalent exposure of about 10^{-9} torr-sec to the oxygen or water molecules. Since from kinetic theory a monolayer of a chemisorbed film requires about 1 to 3 x 10^{-6} torr-sec to form, an exposure of 10^{-9} torr-sec to oxygen or water molecules is not expected to have an effect on cohesion. These considerations suggest that no effect of exposure on the cohesion of copper is expected to occur in the present vacuum environment up to about 10^{-1} torr-sec.

ACKNOWLEDGMENT

The authors wish to acknowledge the assistance of G. Stone in the design and construction of the ultrahigh vacuum mechanical test equipment. They also wish to acknowledge the financial support of this research program by the Office of Naval Research under Contract Nonr-4825(00).

REFERENCES

1. R. W. Roberts and L. E. St. Pierre, "Ultrahigh Vacuum", Science, Vol. 147, No. 3665, 26 March, 1965, p. 1529.

2. R. M. Evans and R. E. Monroe, "Surface Welding in the Space Environment", DMIC Memo 214, June 9, 1966.

3. J. L. Ham, "Metallic Cohesion in High Vacuum", ASLE Trans. Vol. 6, 1963, p. 20.

4. J. L. Ham, "Cohesion of Copper and Steel Repeated Fractured and Rejoined in Vacuum", Soc. Automotive Eng., Preprint 632D, Jan. 14-16, 1963.

5. H. Schwartzbart and W. Brown, "Notch-Bar Tensile Properties of Various Materials and Their Relation to the Unnotched Flow Curve and Notch Sharpness", Trans. ASM, Vol. 46, 1954, p. 998.

6. I. Kramer, H. Shen and S. Podlasek, "The Influence of a Space Environment on the Mechanical Behavior of Metals", Experimental Mechanics, Jan. 1966.

7. H. A. Steinherz and P. A. Redhead, "Ultrahigh Vacuum", Scientific American, Vol. 206, March, 1962, p. 78.

8. M. E. Sikorski, " Correlation of the Coefficient of Adhesion with Various Physical and Mechanical Properties of Metals," Jnl. of Basic Engineering, Vol. 85, 1963 p. 279.

9. M. E. Sikorski, "The Adhesion of Metals and Factors that Influence It," Wear, Vol. 7, 1964, p. 144.

10. J. F. Judge, "Cold Welding Promises Means to Bond Dissimilar Metals," Missiles and Rockets, Apr. 14, 1966, p. 24.

11. N. Brown and K. F. Lukens, "Microstrain in Polycrystalline Metals," Acta Met, Vol. 9, 1961, p. 106.

12. W. D. Brentnall and W. Rostoker, "Some Observations on Microyielding," Acta Met, Vol. 13, 1965, p. 187.

13. H. Conrad, "The Cryogenic Properties of Metals," High Strength Materials, Wiley, 1965, p. 436.

14. H. Conrad, L. Rice and S. Feuerstein, "Effect of Grain Size on the Dislocation Density and the Flow Stress of Niobium," to be published.

15. D. V. Keller, "Applications of Recent Static Adhesion Data to the Adhesion Theory of Friction," presented at Sagamore Conf. on The Physical and Chemical Characteristics of Surfaces," Aug. 23-26, 1966.

16. B. M. W. Trapnell, Chemisorption, Academic Press, 1955, p. 61 and 173.

TABLE I

Condition and Mechanical Properties of the Coppers Used in this Investigation[1]

Condition	Grain Size	Hardness	Atmospheric Pressure				Ultrahigh Vacuum ($2 - 10 \times 10^{-11}$ torr)			
	Microns	VHN 10 Kg	Y.S.[2] Ksi	T.S.[3] Ksi	F.S.[4] Ksi	R.A.[5] %	Y.S.[2] Ksi	T.S.[3] Ksi	F.S.[4] Ksi	R.A.[5] %
I. Tough Pitch										
As-Received (AR) - C.@.	--	79	---	79.7	113.7	31	---	79.8	105.2	28
AR Annealed 1 hr. @ 600°C	9-10	39	15.4	41.5	83.3	59	15.7	41.7	84.4	59
AR Annealed 1 hr. @ 950°C	50	37	13.1	39.3	79.4	59	11.9	38.6	75.5	58
II. OFHC										
As-Received (AR) - C.W.	--	83	---	87.1	198.3	56	---	87.5	184.1	52
AR Annealed 1 hr. @ 350°C	6-7	39	20.6	43.5	142.5	82	27.4	46.8	137.4	77
AR Annealed 1 hr. @ 600°C	100	31	10.9	38.5	124.4	81	15.0	40.9	129.5	79
III. High Purity										
As-Received & Straightened	350	31	23.8	34.3	195.8	92	----	----	----	--
AR Swaged 75%	---	69	---	66.9	318.5	79	----	65.8	272.9	76
AR Annealed 1 hr. @ 600°C	450	28	11.5	36.9	144.5	92	12.0	39.4	162.5	86

(1) Specimen dimensions given in Fig. 4.

(2) Load at 10^{-3} in. plastic elongation divided by initial cross section area at root of notch, A_o.

(3) Maximum load divided by A_o.

(4) Load divided by cross section area at root of notch at fracture, A_F.

(5) Reduction in Area = $\frac{A_o - A_F}{A} \times 100$

TABLE II

Effect of Elastic Modulus on the Cohesion Coefficient α

Metal	Crystal Structure	E 10^6 psi	α Avg.	Ref.	αE 10^6 psi
Cu	FCC	16	0.75	Present	12.0
			0.65	3,4	10.4
Ag	FCC	11	0.84	15	9.2
Fe	BCC	29	0.35	3,4	10.2

LIST OF FIGURES

14. Effect of compression stress on the cohesion stress for various coppers.

15. Effect of compression stress on the cohesion coefficient for various coppers.

16. Effect of exposure to the vacuum environment on the cohesion coefficient α_o.

17. Amplitude of transmitted ultrasonic wave versus cohesion ratio for tough pitch copper.

18. Unetched cross-section of cold welded tough pitch copper (10μ g.s.) specimen

    (a) $L_c/L_{F_o} = 0.5$ (b) $L_c/L_{F_o} = 1.0$ Mag 60X.

19. Microstructure of cold welded ($L_c/L_{F_o} = 1.0$) tough pitch copper (10μ g.s.) specimen. $FeCl_3$ etch.

20. Microstructure of cold welded ($L_c/L_{F_o} = 1.0$) OFHC copper (7μ g.s.) specimen. $FeCl_3$ etch.

21. Microstructure of cold welded ($Lc/L_{F_o} = 1.0$) OFHC copper (100μ g.s.) specimen. $FeCl_3$ etch.

22. Cohesion ratio versus square of the compression ratio.

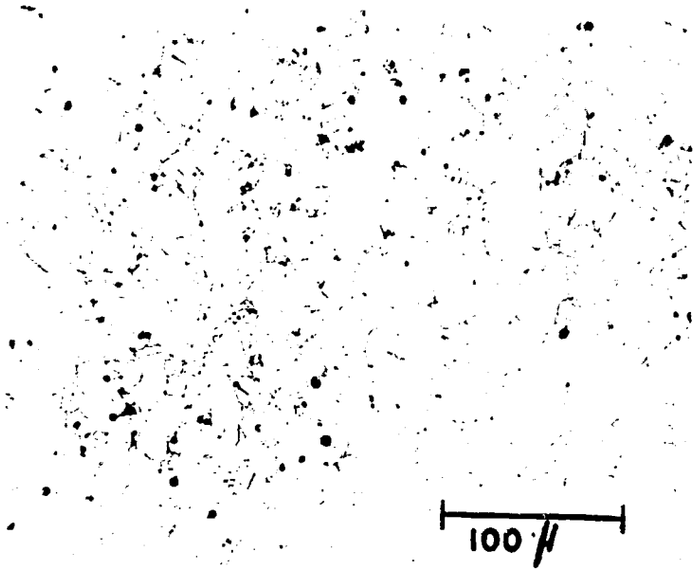

a.

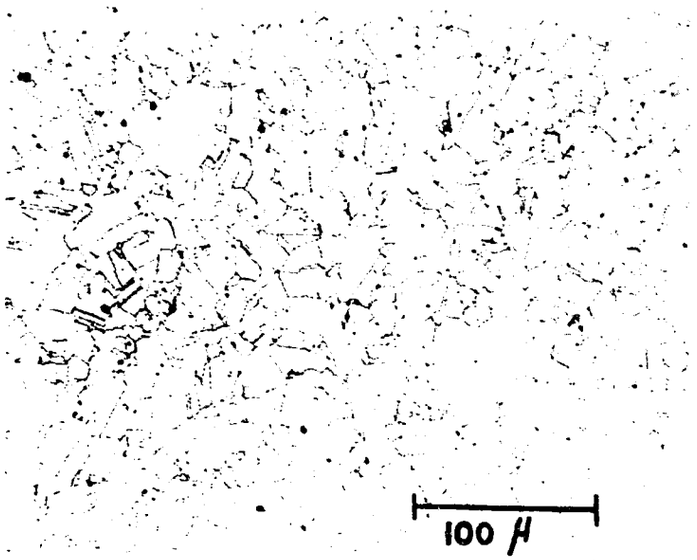

b.

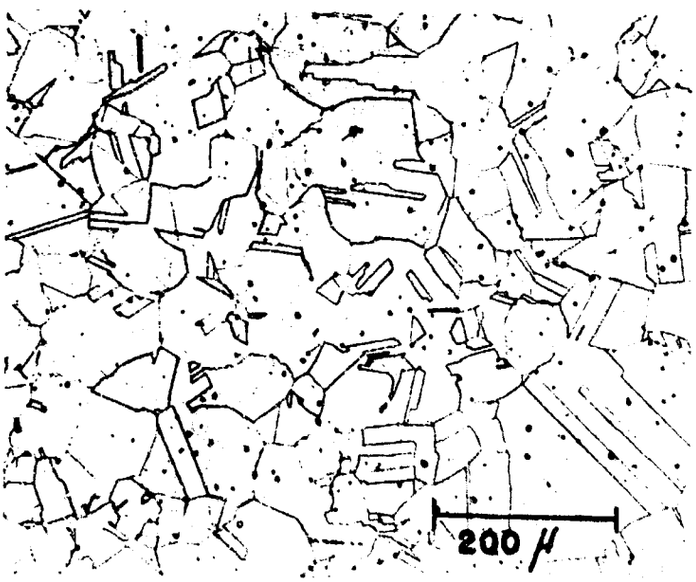

c.

Figure 1

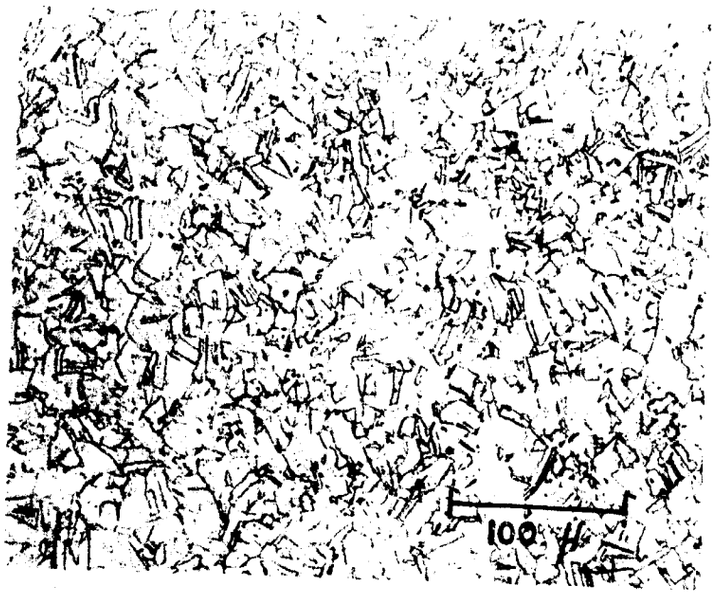

a.

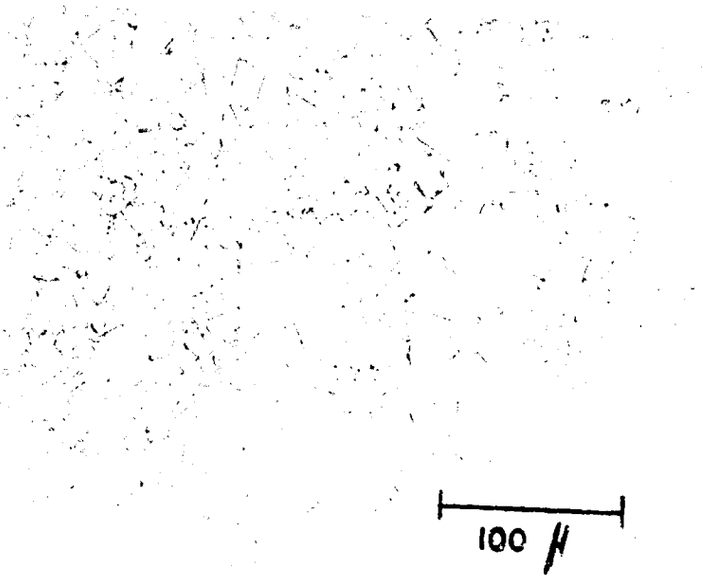

b.

c.

Figure 2

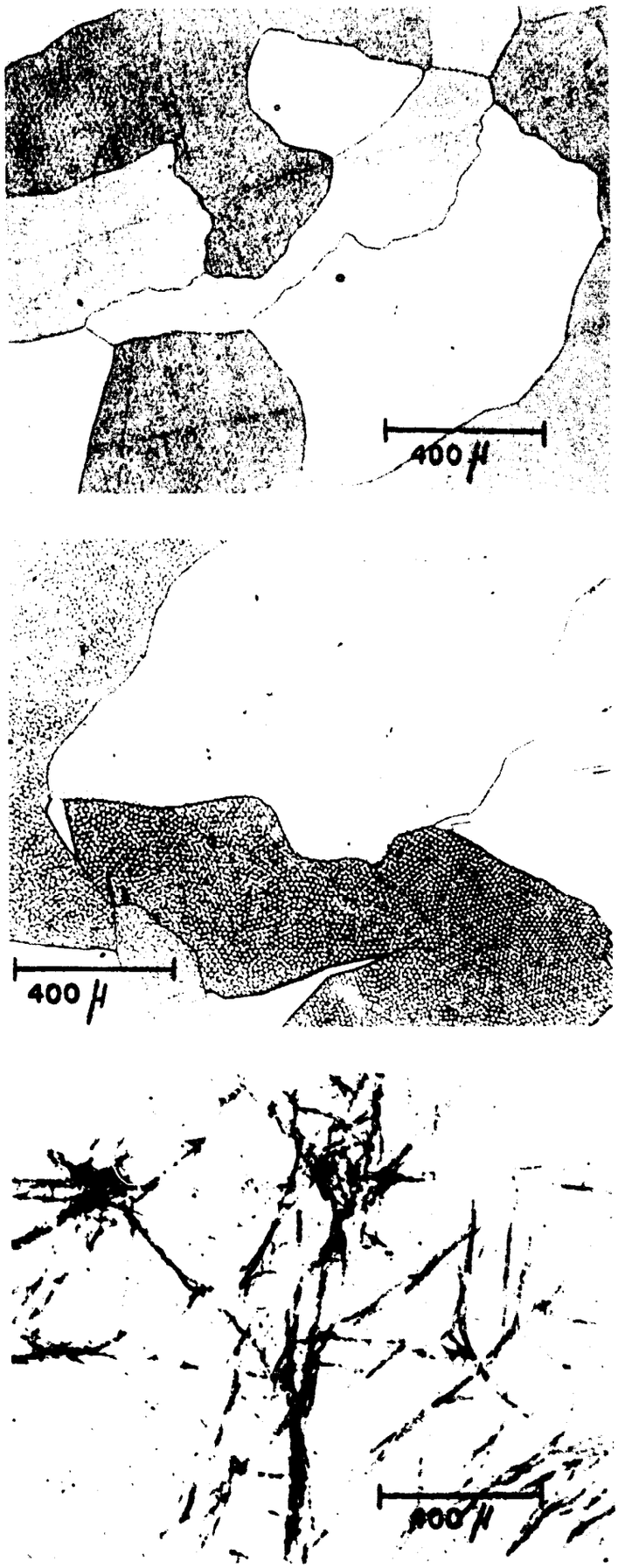

Figure 3

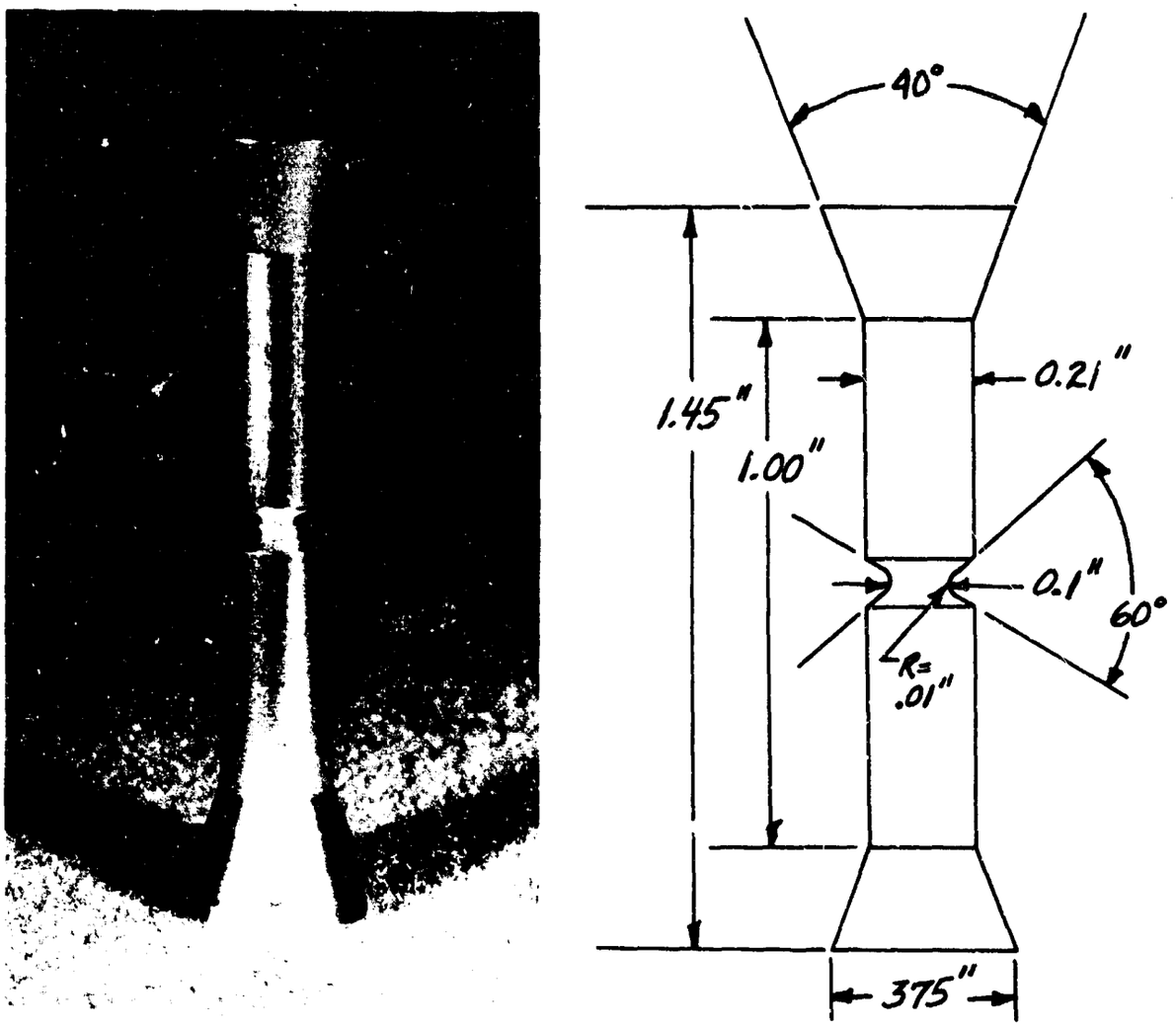

Specimen employed in present tests.
Left: photograph of actual specimen; Right: dimensions of specimen.

Figure 4

SCHEMATIC OF ULTRA-HIGH VACUUM TEST EQUIPMENT

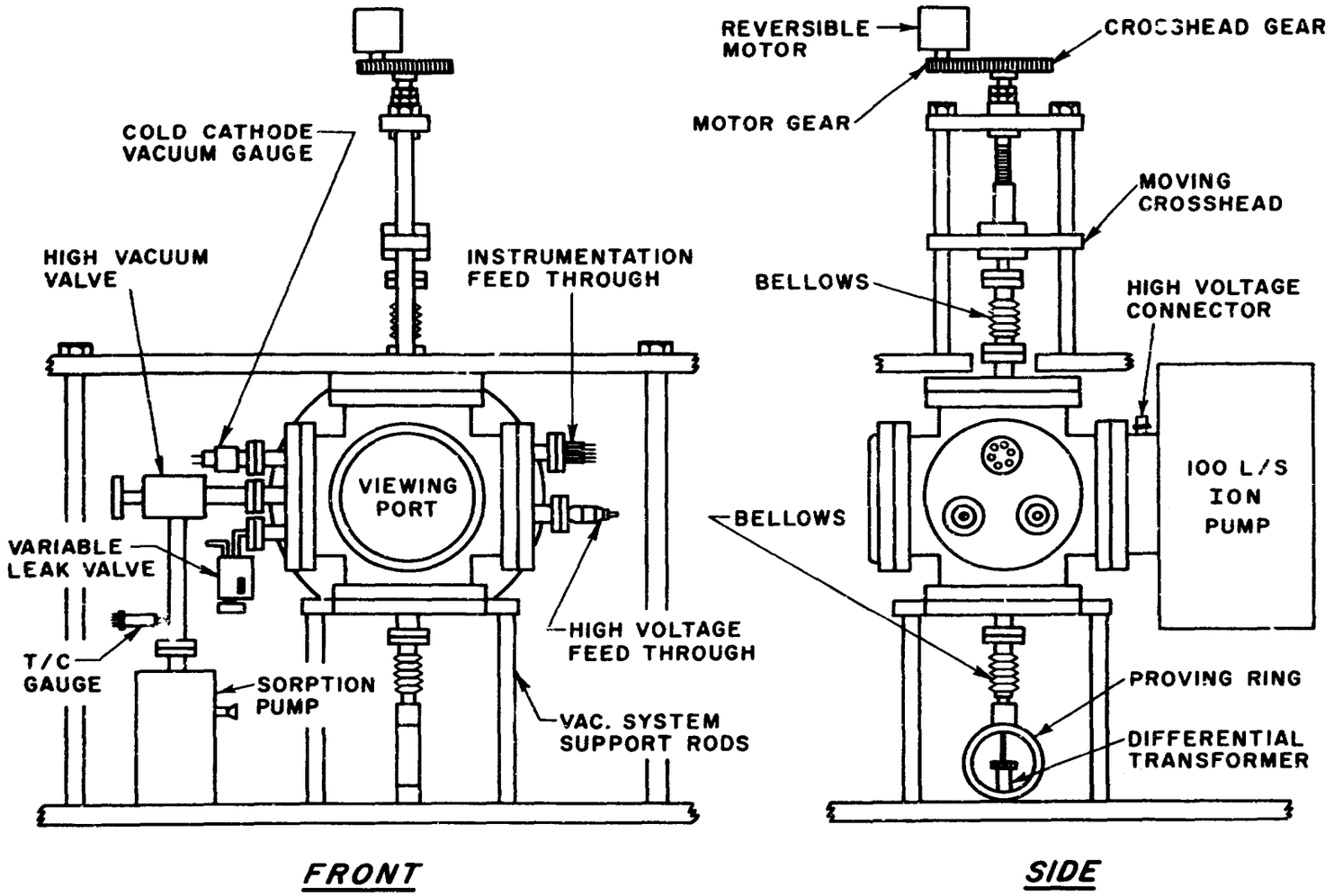

Figure 5

SCHEMATIC OF SPECIMEN GRIPS AND ALIGNMENT FIXTURE

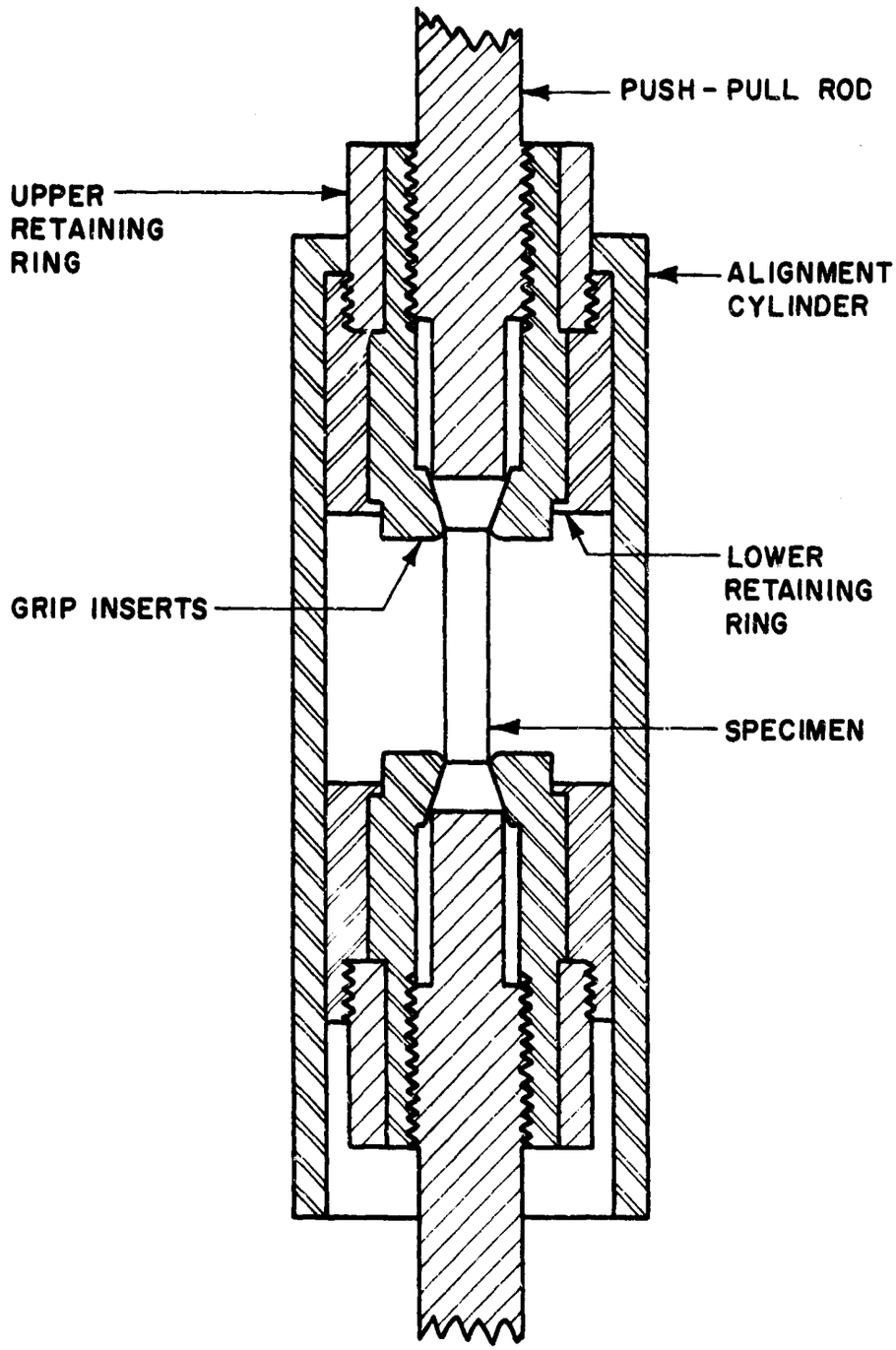

Figure 6

LOAD - CROSSHEAD TRAVEL CURVES FOR INITIAL FRACTURE, COLD WELDING AND SUBSEQUENT FRACTURE OF WELD FOR AS-RECEIVED TOUGH PITCH COPPER

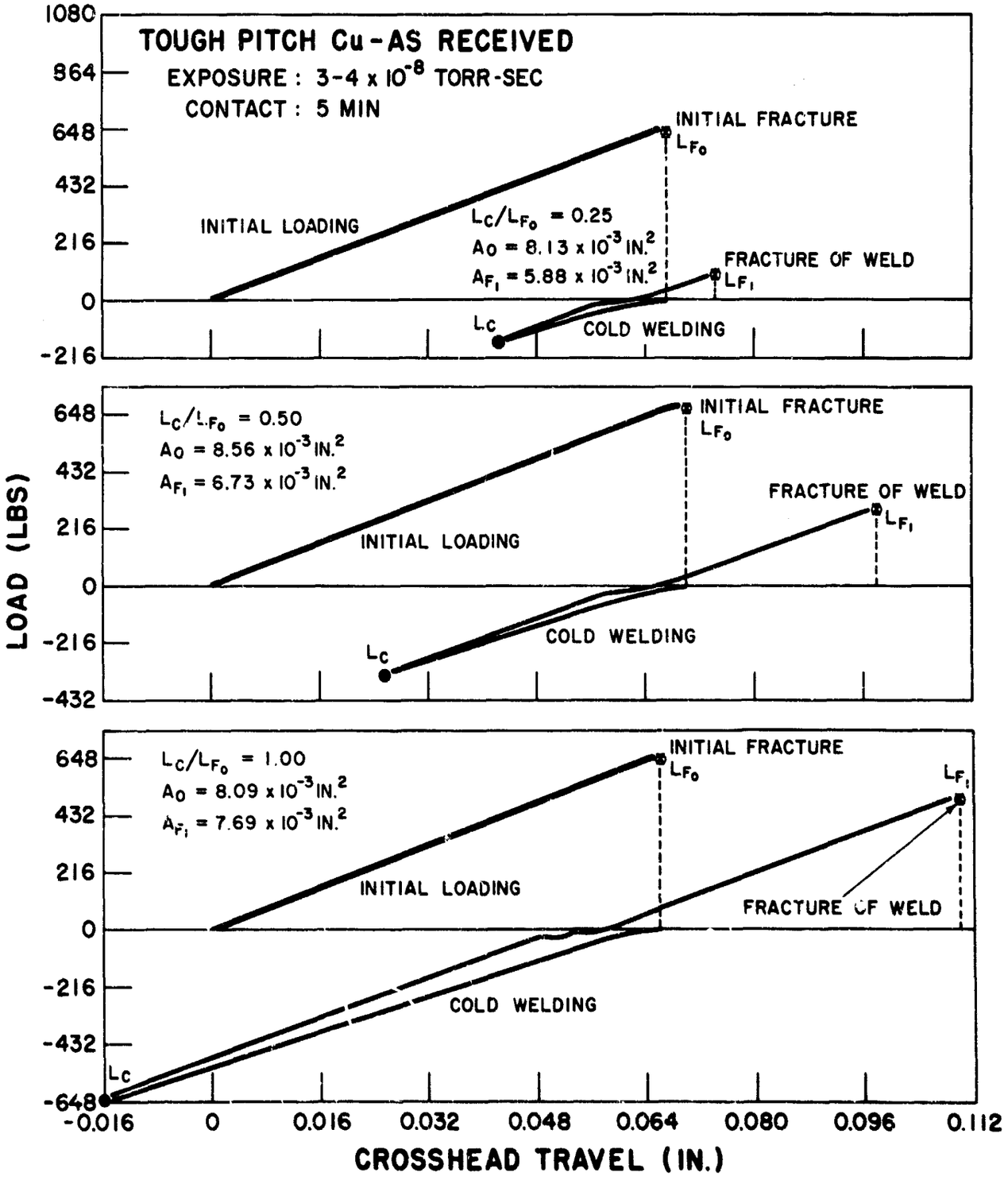

Figure 7

LOAD - CROSSHEAD TRAVEL CURVES FOR INITIAL FRACTURE, COLD WELDING AND SUBSEQUENT FRACTURE OF WELD FOR ANNEALED TOUGH PITCH COPPER OF 10μ GRAIN SIZE

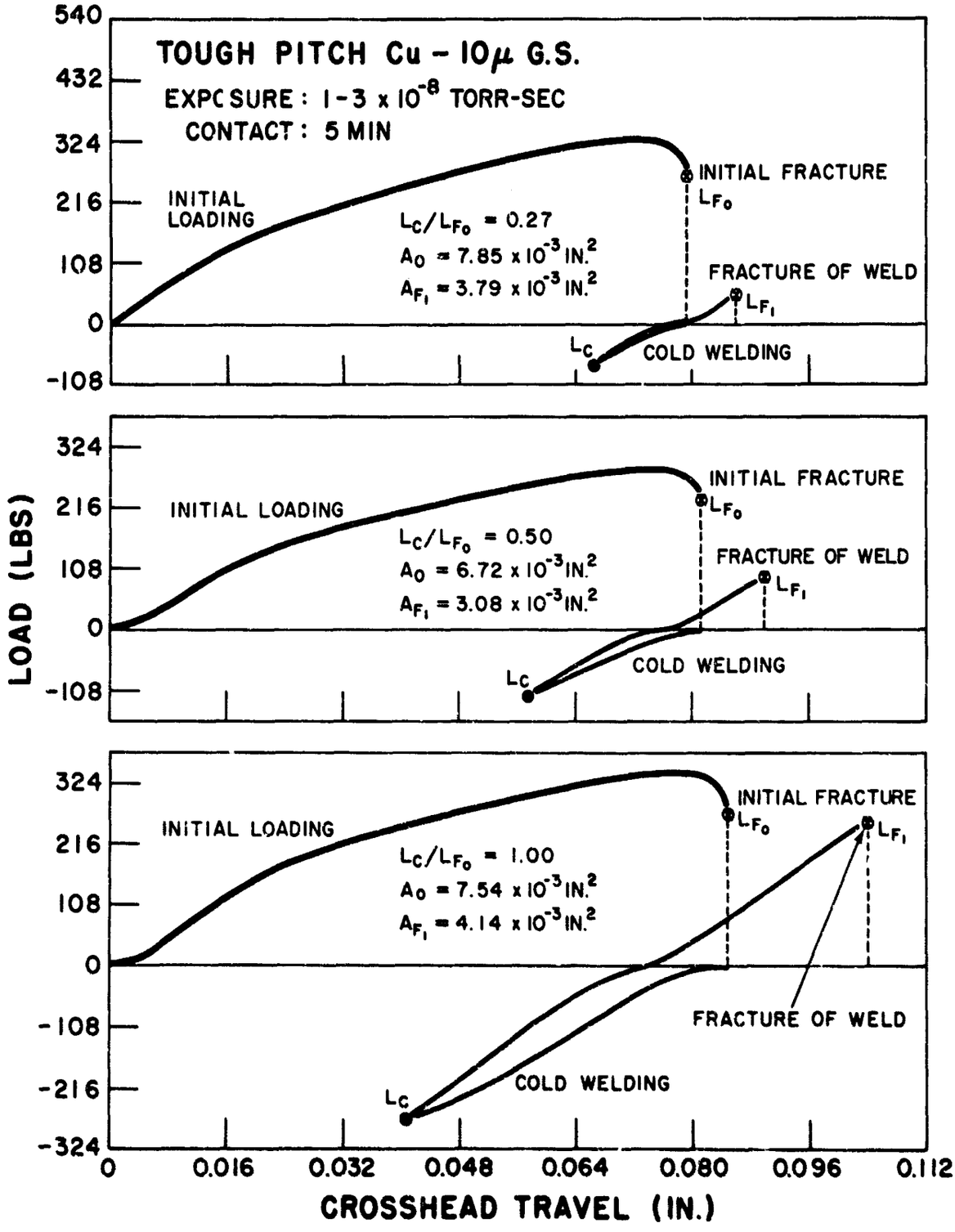

Figure 8

LOAD - CROSSHEAD TRAVEL CURVES FOR INITIAL FRACTURE, COLD WELDING AND SUBSEQUENT FRACTURE OF WELD FOR ANNEALED OFHC COPPER OF 7μ GRAIN SIZE

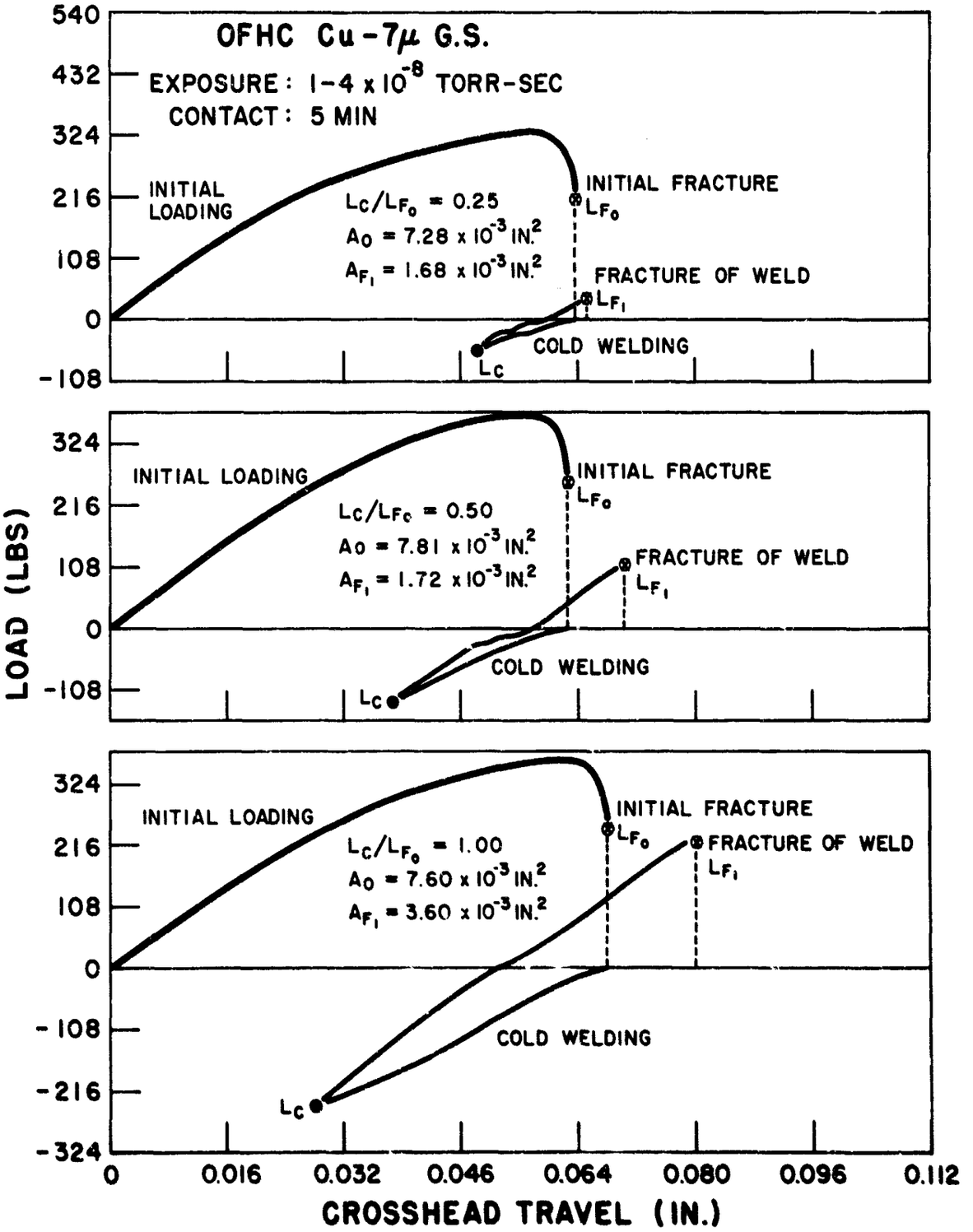

Figure 9

EFFECT OF COMPRESSION RATIO ON THE PLASTIC COMPONENT OF THE CONTRACTION DURING COLD WELDING

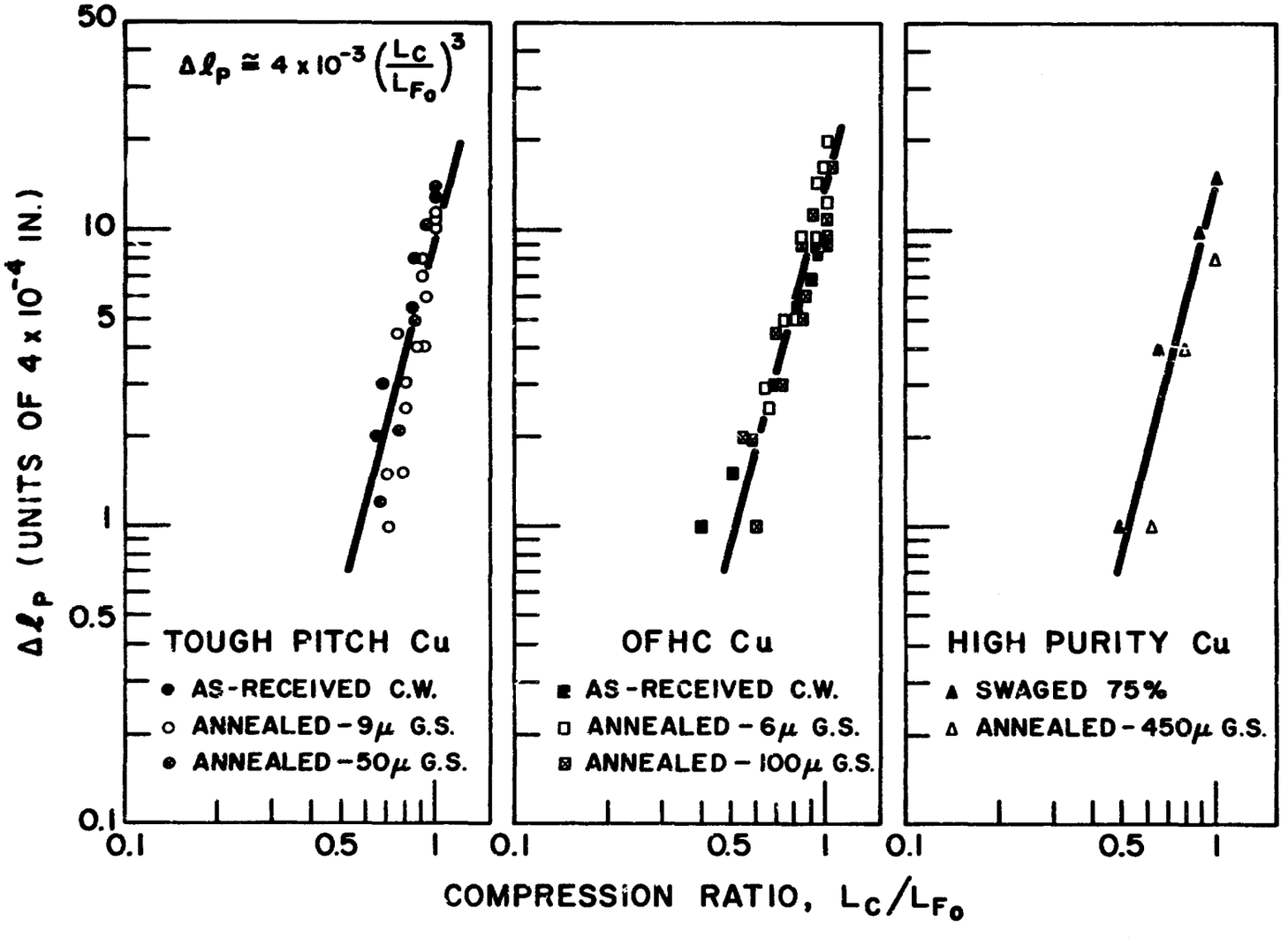

Figure 10

COHESION RATIO VERSUS COMPRESSION RATIO
FOR TOUGH PITCH COPPER

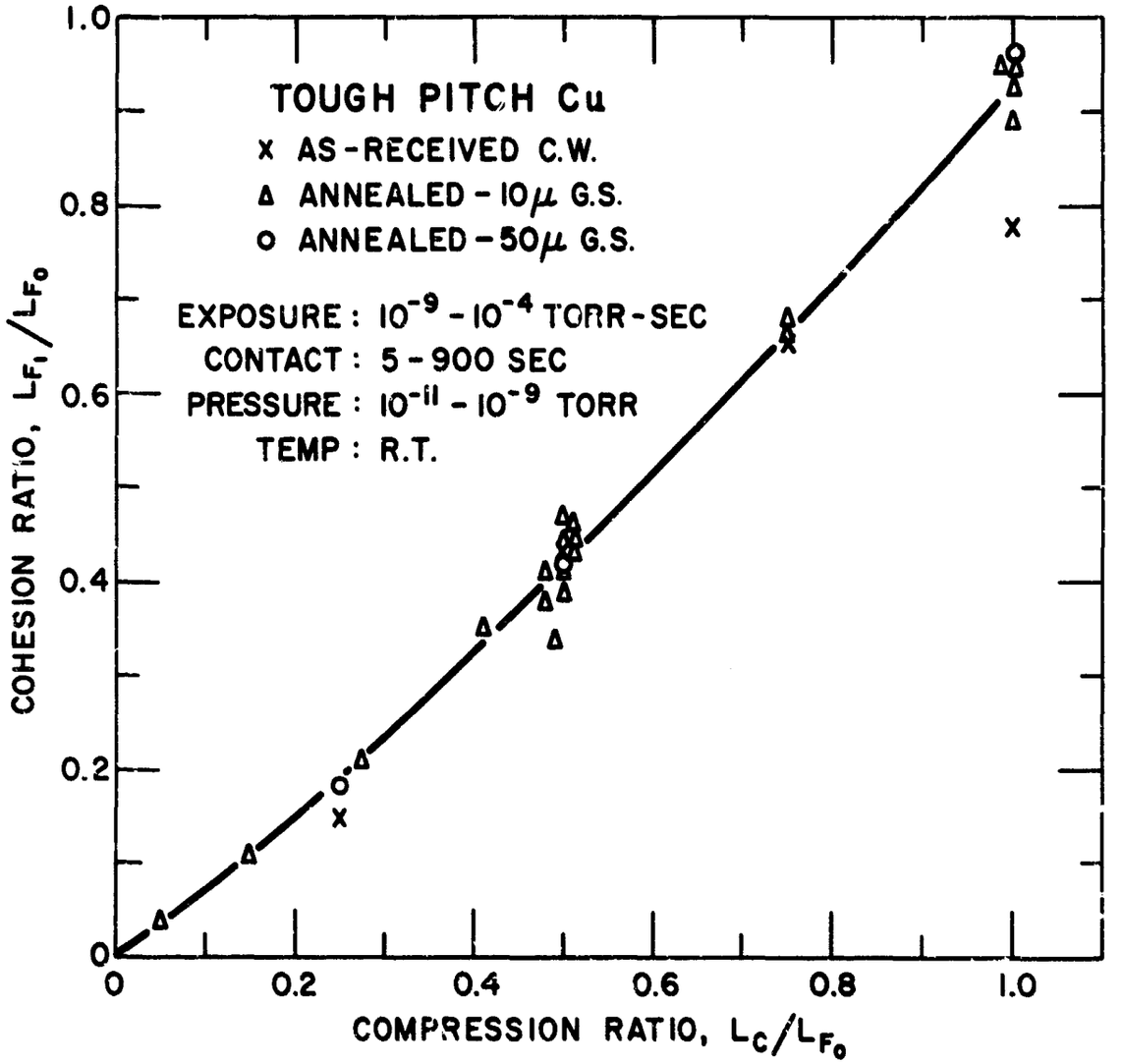

Figure 11

EFFECT OF COMPRESSION RATIO ON THE COHESION RATIO

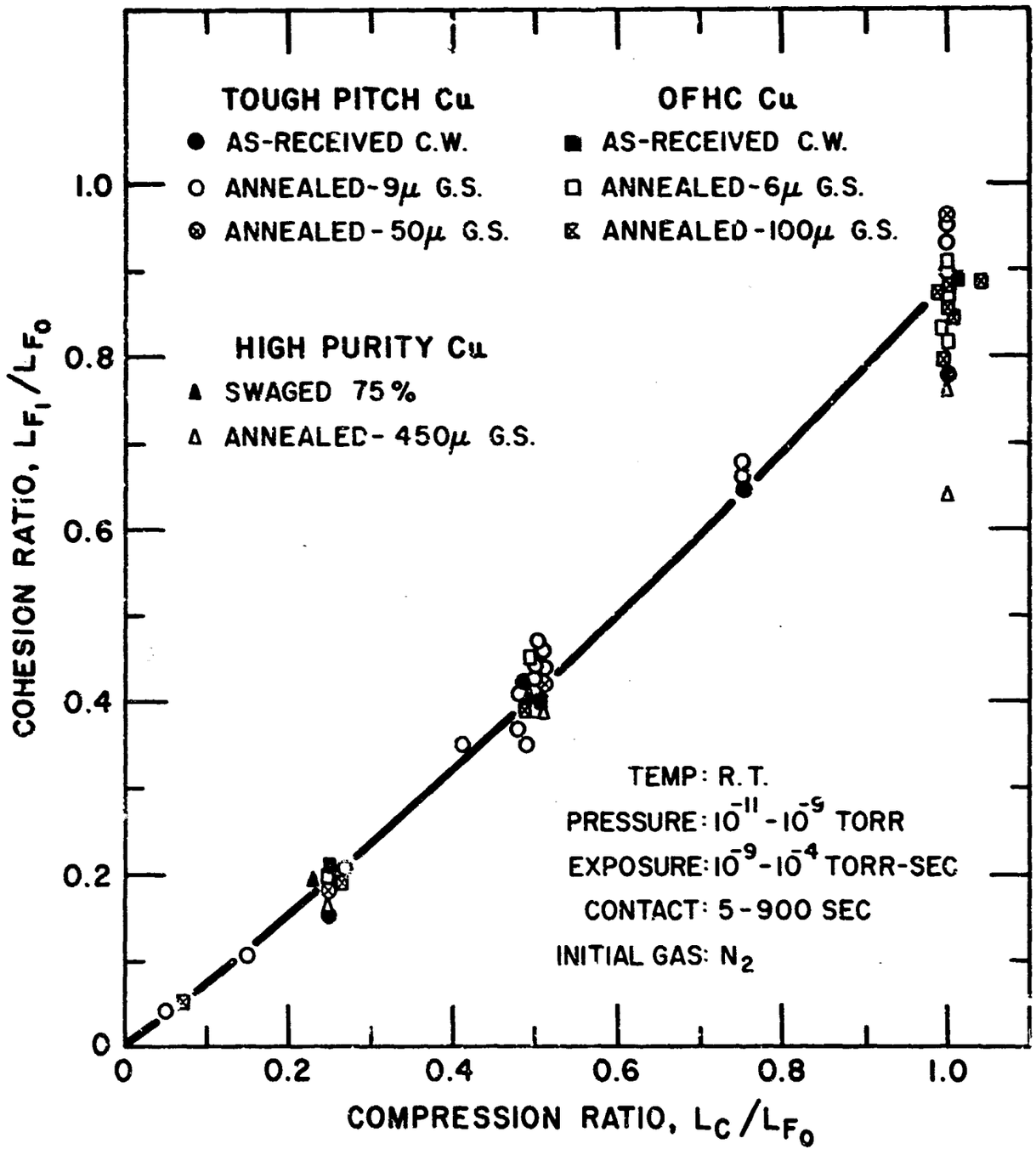

Figure 12

EFFECT OF COMPRESSION RATIO ON THE COHESION COEFFICIENT

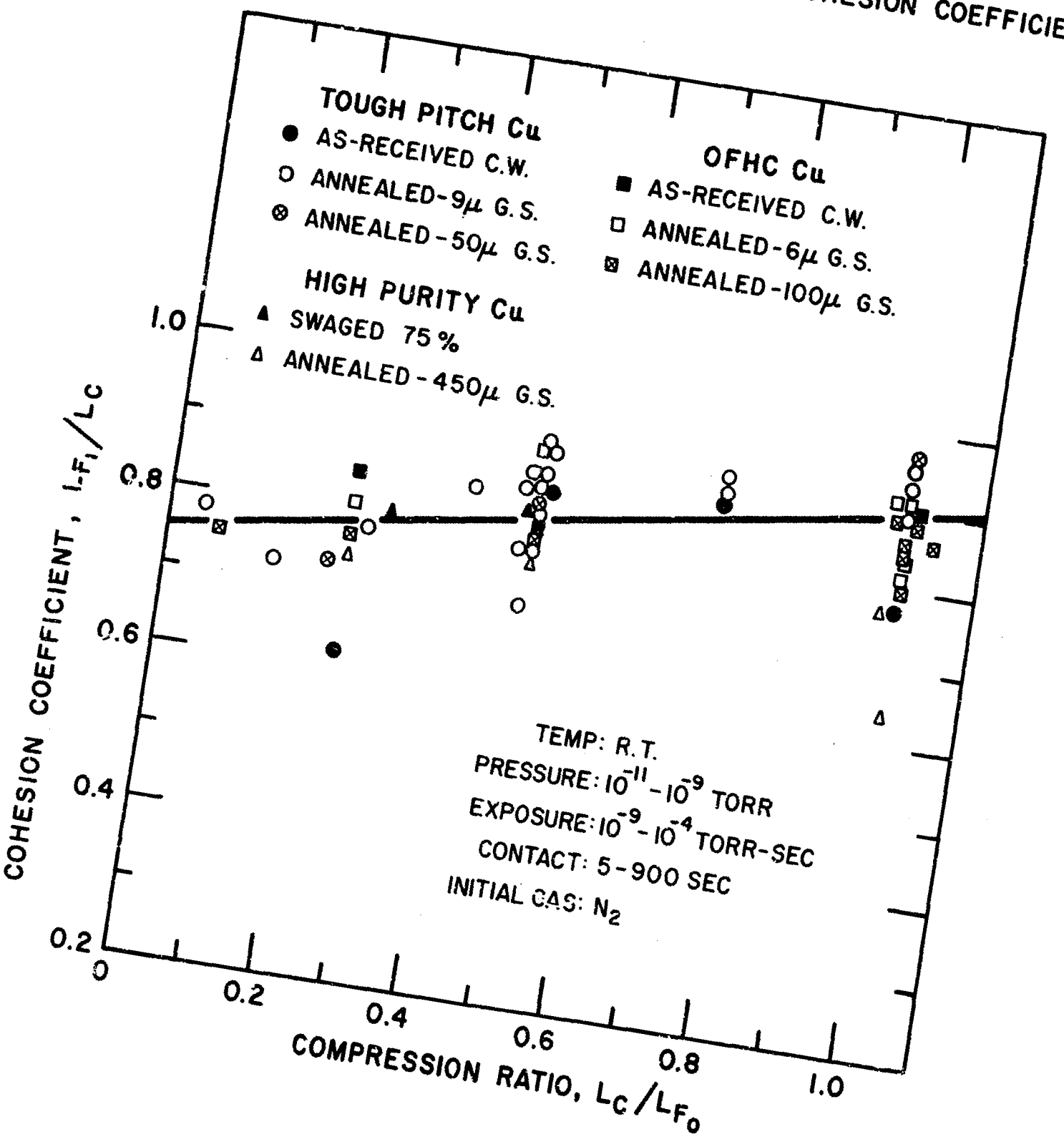

Figure 13

EFFECT OF COMPRESSION STRESS ON THE COHESION STRESS

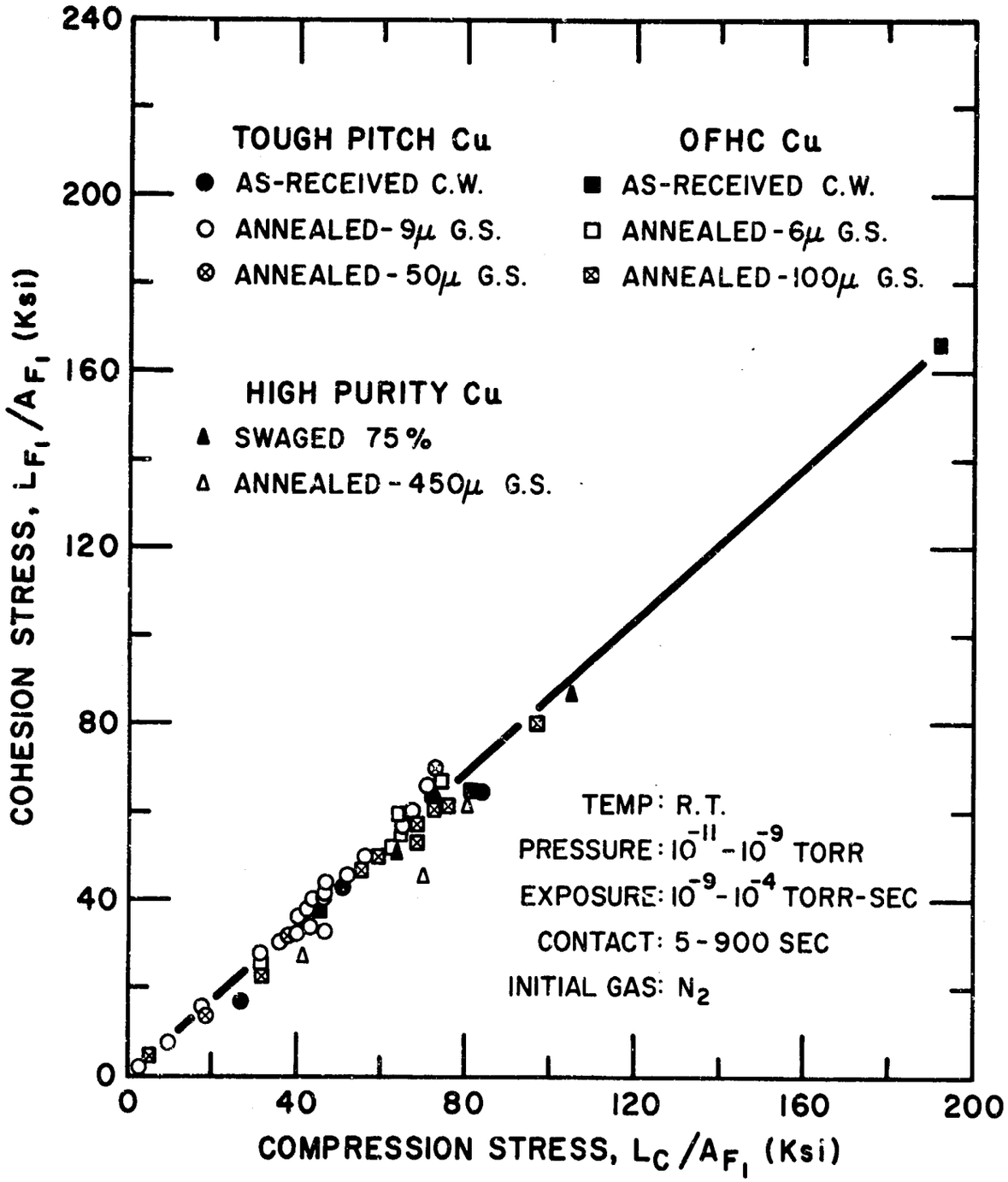

Figure 14

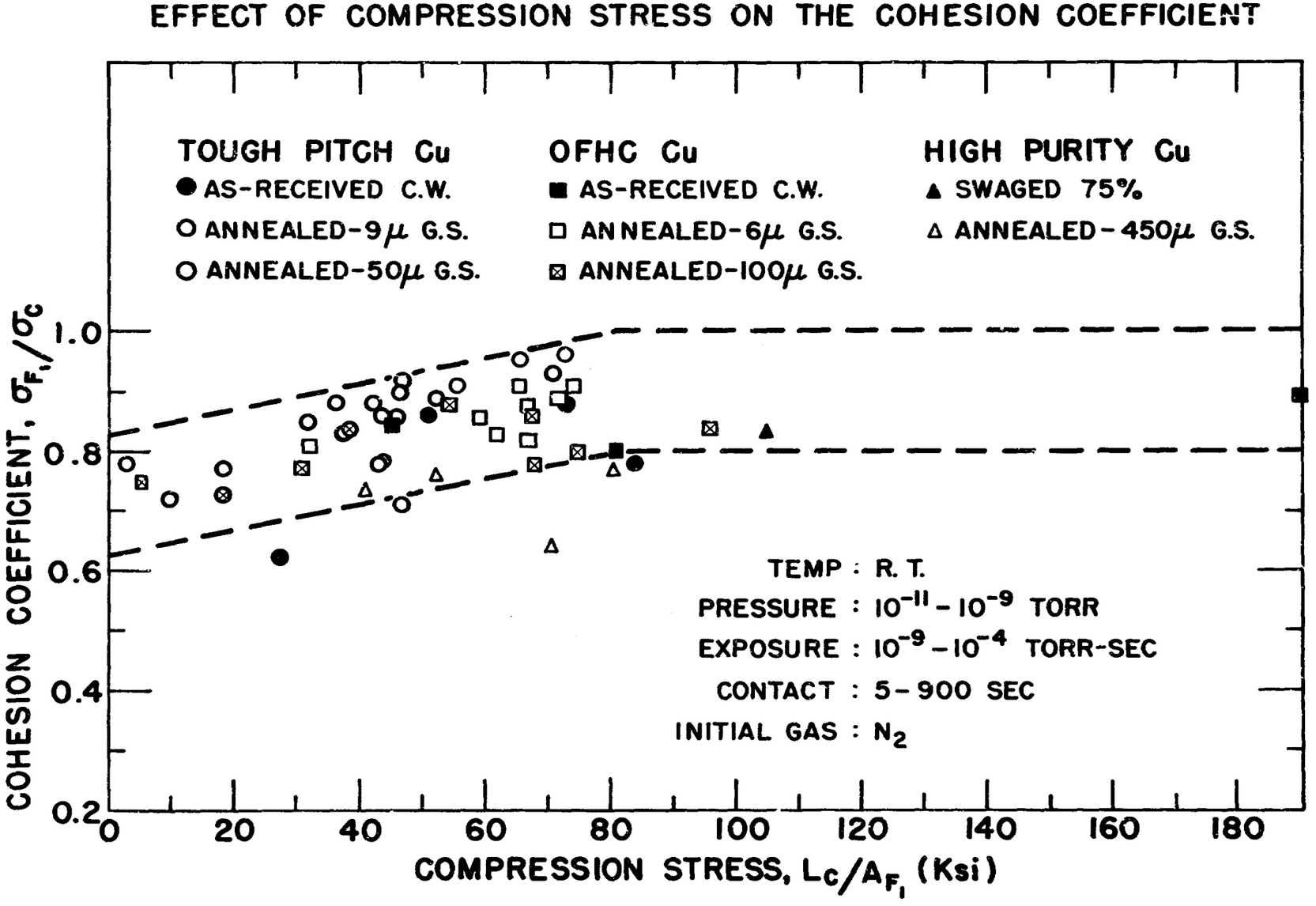
EFFECT OF COMPRESSION STRESS ON THE COHESION COEFFICIENT
TOUGH PITCH Cu
● AS-RECEIVED C.W.
○ ANNEALED-9μ G.S.
○ ANNEALED-50μ G.S.
OFHC Cu
■ AS-RECEIVED C.W.
□ ANNEALED-6μ G.S.
⊠ ANNEALED-100μ G.S.
HIGH PURITY Cu
▲ SWAGED 75%
△ ANNEALED-450μ G.S.
TEMP : R. T.
PRESSURE : $10^{-11} - 10^{-9}$ TORR
EXPOSURE : $10^{-9} - 10^{-4}$ TORR-SEC
CONTACT : 5-900 SEC
INITIAL GAS : N_2
COHESION COEFFICIENT, σ_{F_1}/σ_c
1.0
0.8
0.6
0.4
0.2
0
20
40
60
80
100
120
140
160
180
COMPRESSION STRESS, L_c/A_{F_1} (Ksi)

Figure 15

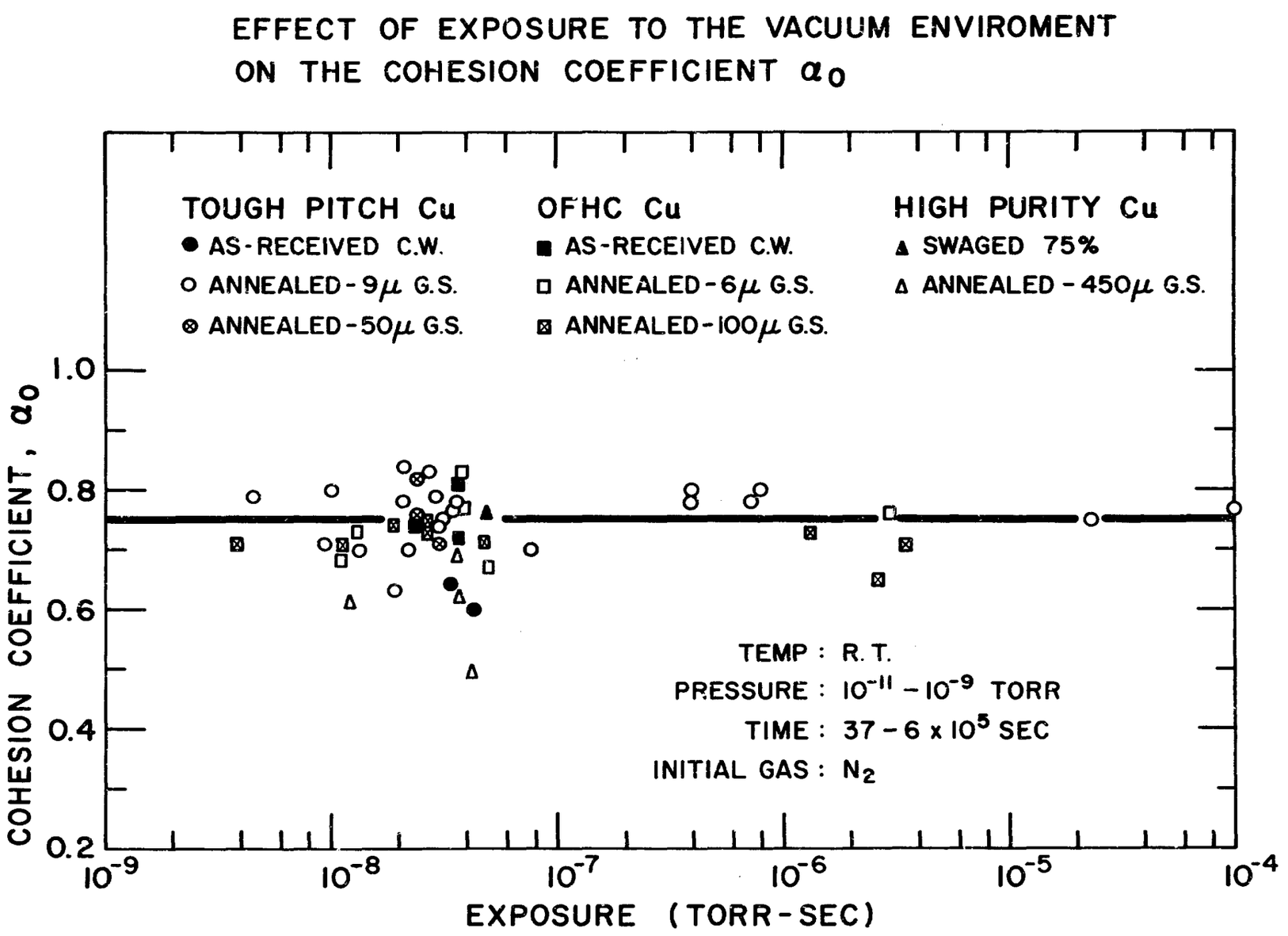
EFFECT OF EXPOSURE TO THE VACUUM ENVIROMENT
ON THE COHESION COEFFICIENT α_0
TOUGH PITCH Cu
● AS-RECEIVED C.W.
○ ANNEALED - 9μ G.S.
⊗ ANNEALED - 50μ G.S.
OFHC Cu
■ AS-RECEIVED C.W.
□ ANNEALED - 6μ G.S.
⊠ ANNEALED - 100μ G.S.
HIGH PURITY Cu
▲ SWAGED 75%
△ ANNEALED - 450μ G.S.
TEMP : R.T.
PRESSURE : $10^{-11} - 10^{-9}$ TORR
TIME : $37 - 6 \times 10^5$ SEC
INITIAL GAS : N_2
COHESION COEFFICIENT, α_0
1.0
0.8
0.6
0.4
0.2
10^{-9}
10^{-8}
10^{-7}
10^{-6}
10^{-5}
10^{-4}
EXPOSURE (TORR-SEC)

Figure 16

AMPLITUDE OF TRANSMITTED ULTRASONIC WAVE VERSUS COHESION RATIO FOR TOUGH PITCH COPPER

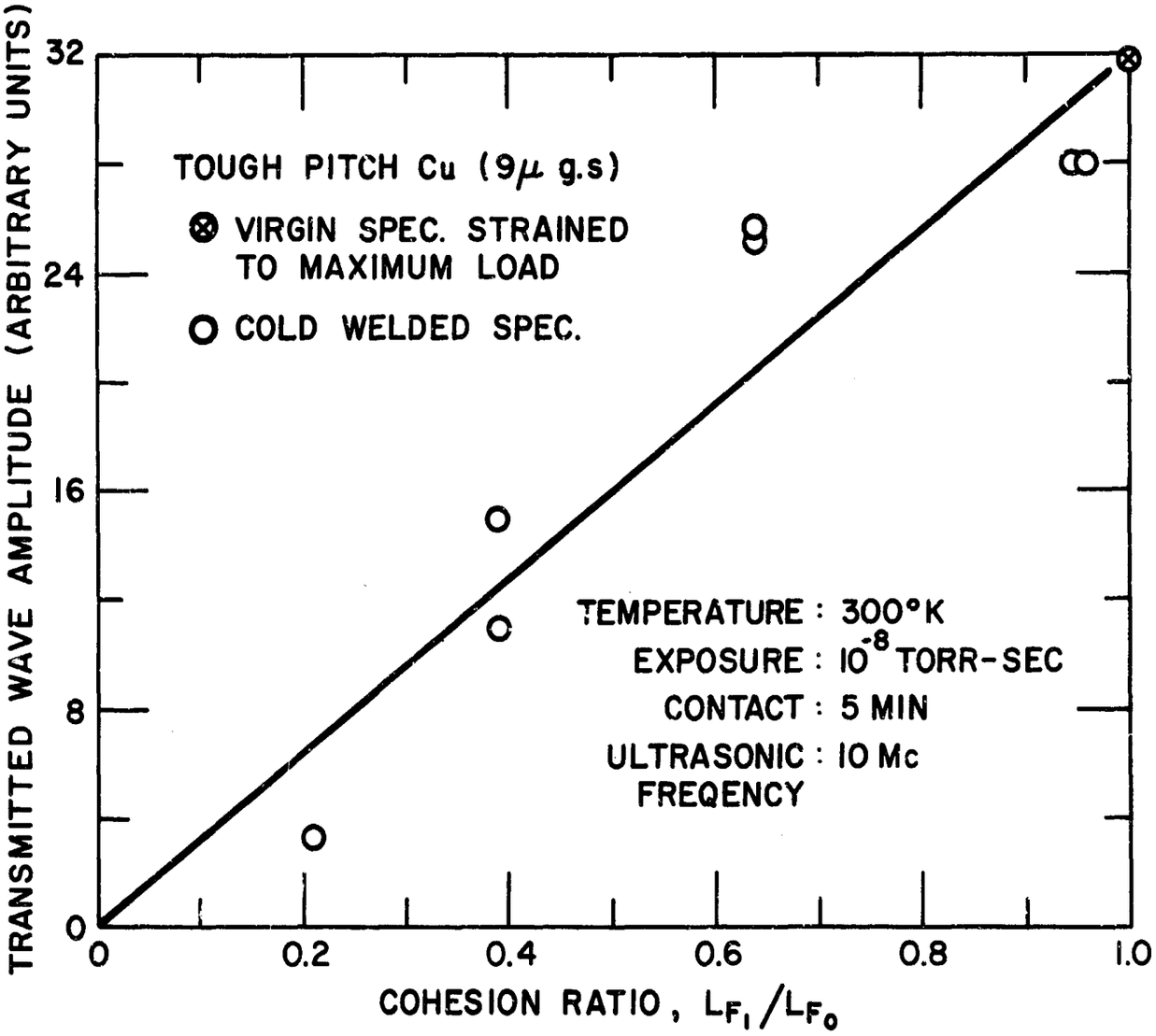

Figure 17

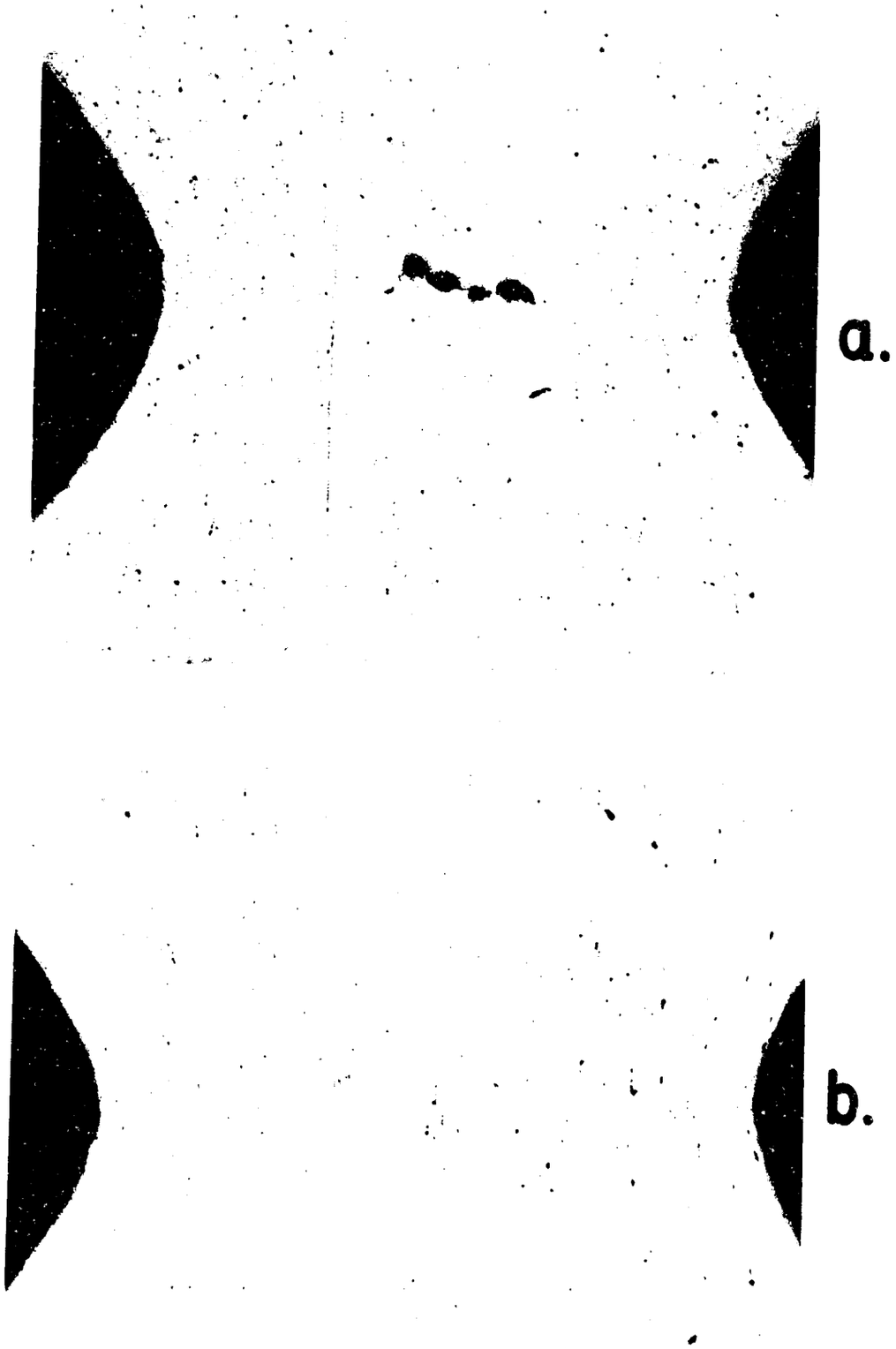

Figure 18

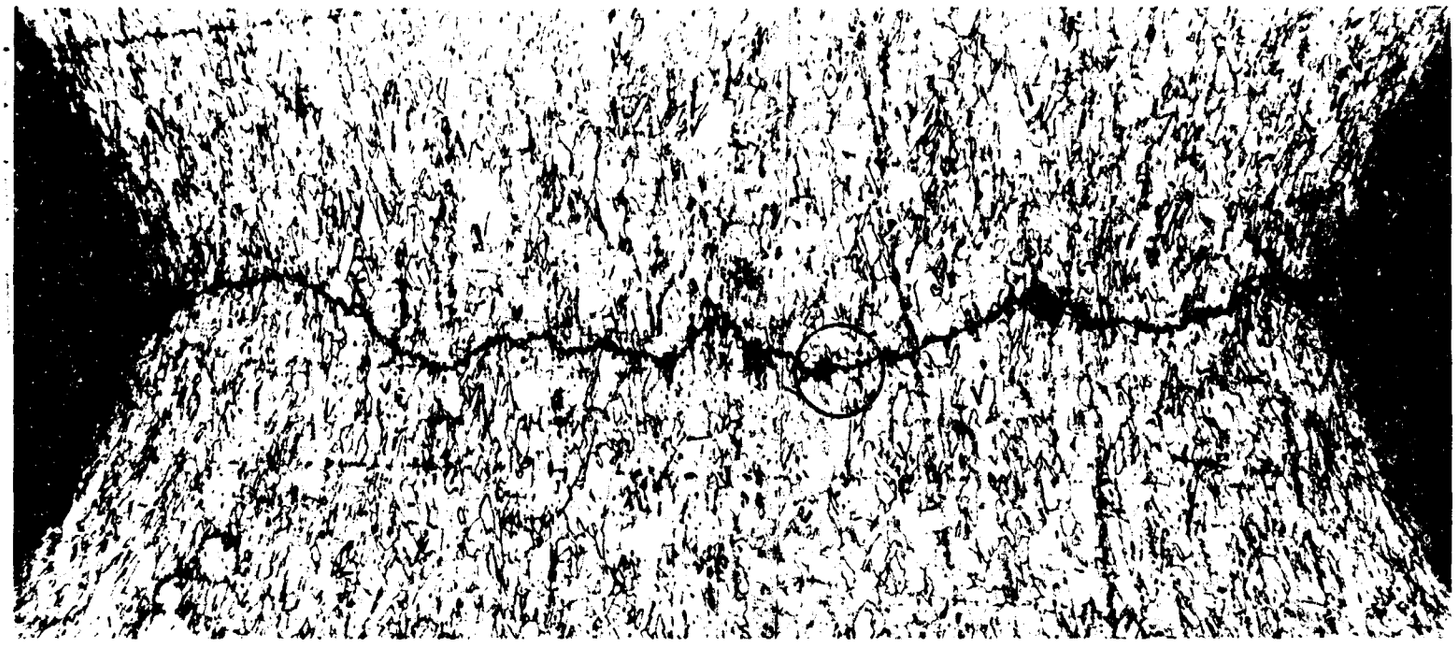

120X

960X

Figure 19

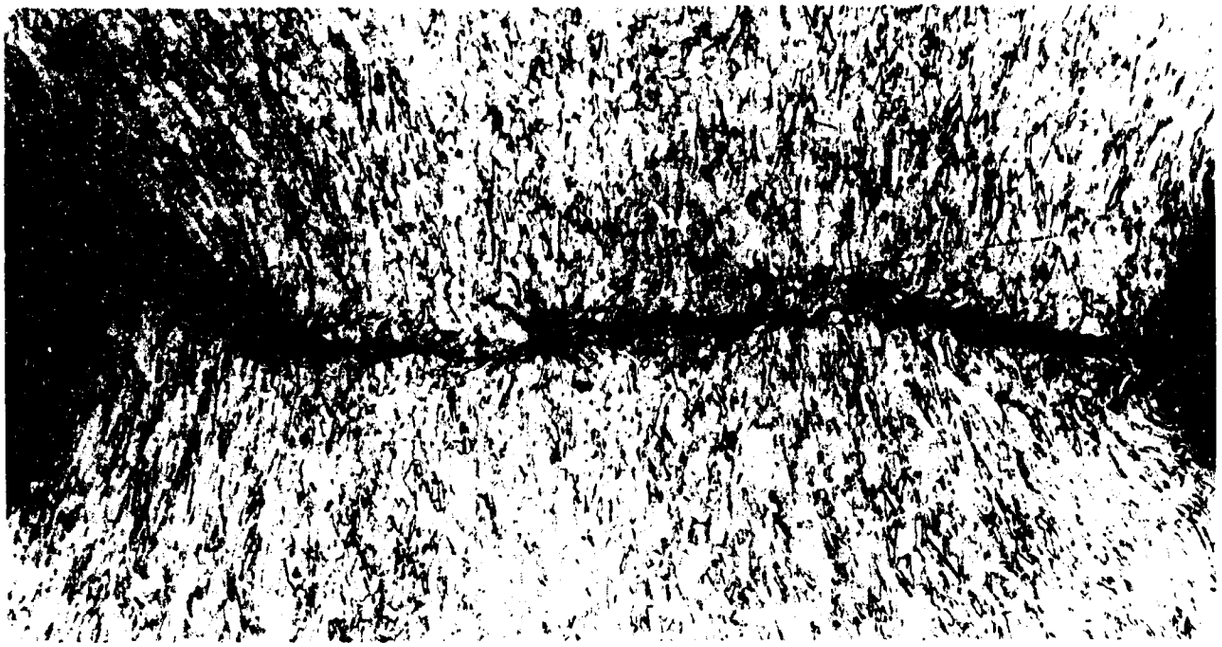

120X

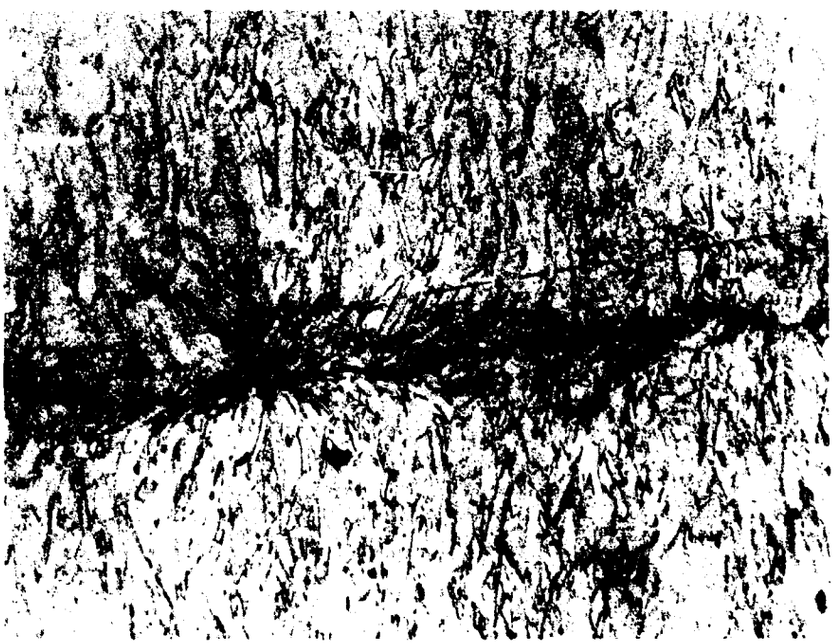

240X

Figure 20

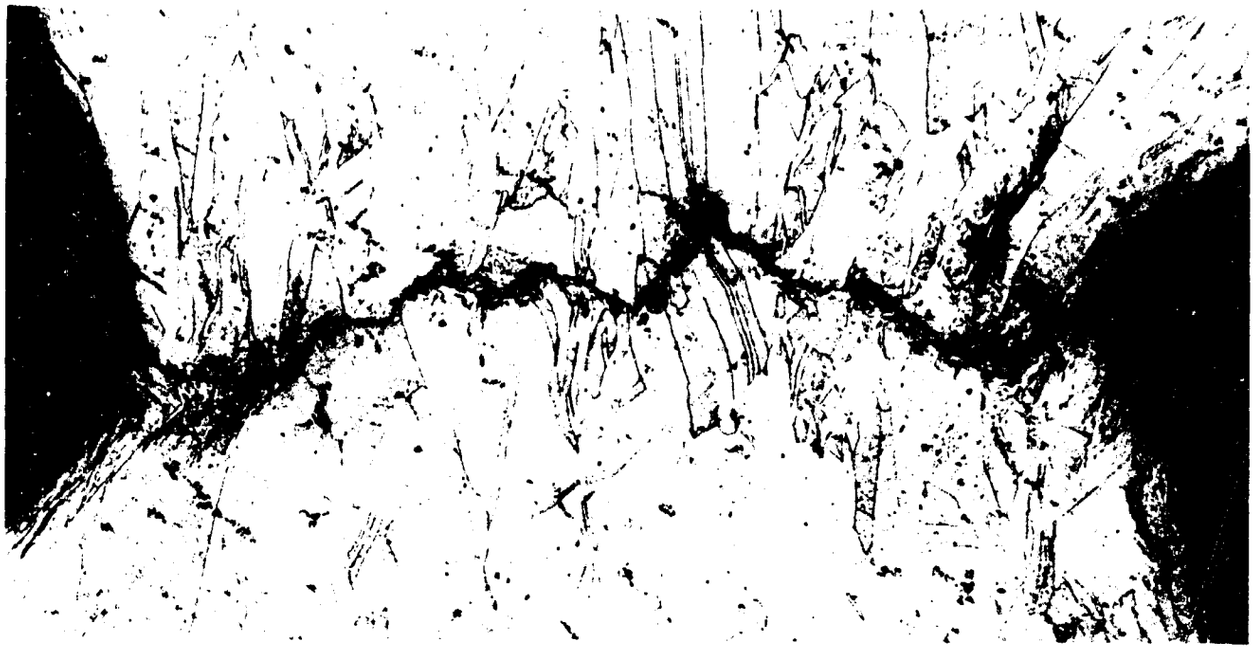

120X

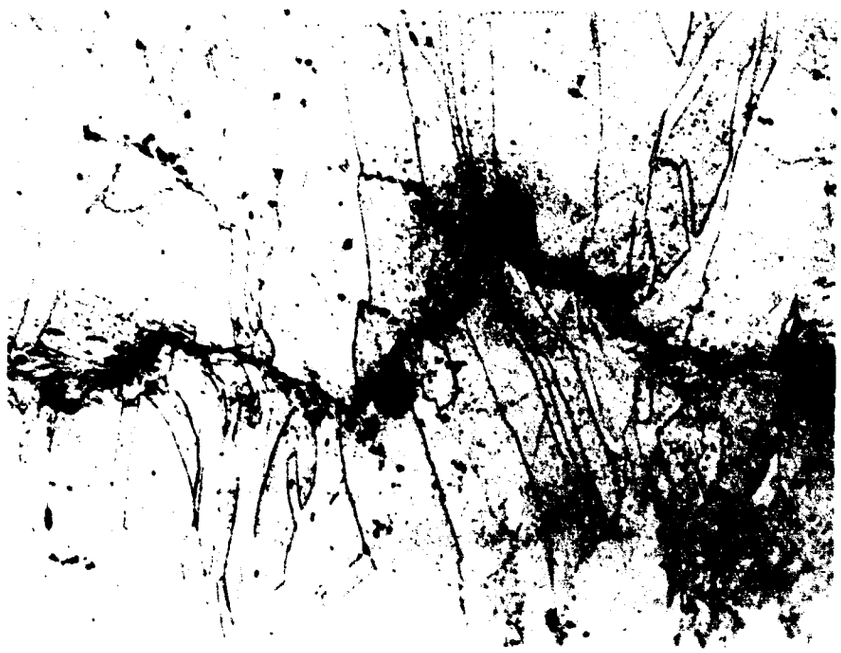

240X

Figure 21

COHESION RATIO VERSUS SQUARE OF THE COMPRESSION RATIO

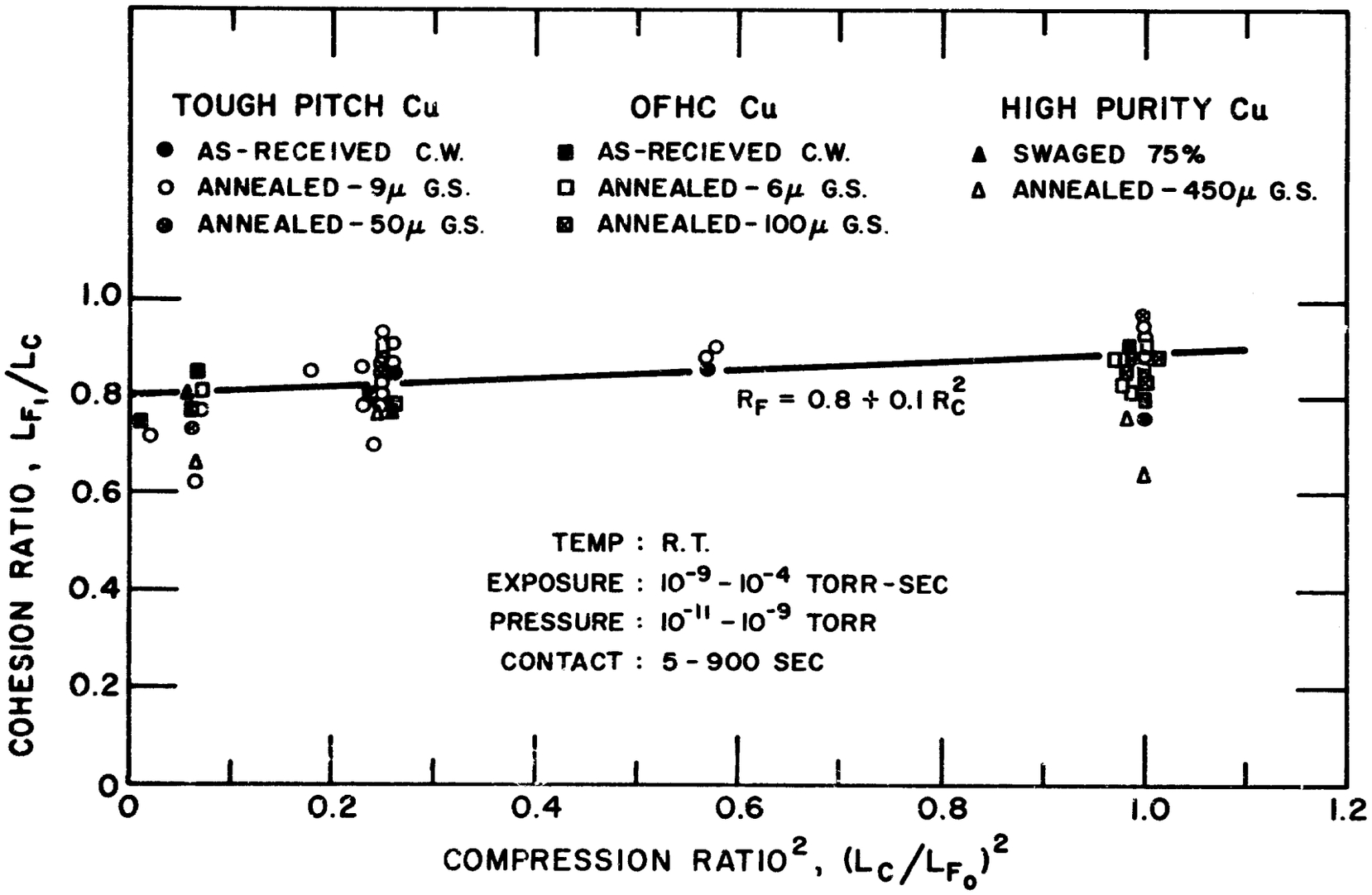

Figure 22